

Article

Climate and Vegetation Change, Hillslope Soil Erosion, and the Complex Nature of Late Quaternary Environmental Transitions, Eastern Mojave Desert, USA

Joseph R. McAuliffe ^{1,*}, Leslie D. McFadden ², Lyman P. Persico ³ and Tammy M. Rittenour ⁴ 

¹ Department of Research, Conservation & Collections, Desert Botanical Garden, 1201 N. Galvin Pkwy., Phoenix, AZ 85008, USA

² Department of Earth & Planetary Sciences, University of New Mexico, Albuquerque, NM 87131, USA

³ Geology Department, Whitman College, Walla Walla, WA 99362, USA

⁴ Department of Geosciences, Utah State University, Logan, UT 84322, USA

* Correspondence: jmcauliffe@dbg.org



Citation: McAuliffe, J.R.; McFadden, L.D.; Persico, L.P.; Rittenour, T.M. Climate and Vegetation Change, Hillslope Soil Erosion, and the Complex Nature of Late Quaternary Environmental Transitions, Eastern Mojave Desert, USA. *Quaternary* **2022**, *5*, 43. <https://doi.org/10.3390/quat5040043>

Academic Editor: James B. Innes

Received: 10 September 2022

Accepted: 10 October 2022

Published: 14 October 2022

Publisher's Note: MDPI stays neutral with regard to jurisdictional claims in published maps and institutional affiliations.



Copyright: © 2022 by the authors. Licensee MDPI, Basel, Switzerland. This article is an open access article distributed under the terms and conditions of the Creative Commons Attribution (CC BY) license (<https://creativecommons.org/licenses/by/4.0/>).

Abstract: In what are now the warm deserts of the American Southwest, direct effects of changing climate on plant distributions are typically viewed as the principal driver of vegetation changes that followed the late Pleistocene–Holocene transition (LPH). However, at a semi-arid site in the eastern Mojave Desert, the transition to modern, shrub-dominated desert scrub on xeric, south-aspect hillslopes occurred only after the erosion of relatively thick soils toward the end of the mid-Holocene. Soils with well-developed Bt horizons began to form in the late Pleistocene on both north- and south-aspect hillslopes through the entrapment and accumulation of aeolian sediments in coarse colluvium. Those soils are capable of absorbing and retaining substantial moisture and support relatively dense stands of perennial C₄ grasses that have diffuse, fibrous root systems. The age of alluvial deposits on the basin floor indicates a surge in sediment production through the erosion of some of those hillslope soils toward the end of the mid-Holocene. However, that erosion was largely limited to the more xeric, more sparsely vegetated, south-aspect hillslopes. The soils formed on mesic north-aspect hillslopes remain largely non-eroded to the present day, demonstrating the central role of vegetation in modulating erosion and sediment supply. The loss of soils from south-aspect hillslopes fundamentally changed the capacity of those environments to absorb and store moisture, and altered the depth and temporal durations of plant-available moisture. Those hydrological changes drove a loss of perennial C₄ grasses and a transition to dominance by xerophytic plants—shrubs with deeper taproots capable of extracting moisture stored within bedrock joints and fractures, and shallow-rooted succulent plants that store moisture internally. Following the LPH, vegetation change at the site apparently occurred in two distinct phases separated in time: (1) initial vegetation changes driven directly by increasing climatic aridity and (2) subsequent changes linked to the later episode of soil erosion. Although climate shifts ultimately generate vegetation changes, the proximate mechanisms to which plants directly respond can lag far behind climatic transitions and involve complex relationships of vegetation, soils, and changing soil hydrologic conditions.

Keywords: climate change; Pleistocene–Holocene transition; soil erosion; vegetation change; woodrat middens; Quaternary palaeoecology

1. Introduction

Major changes in climate during the late Pleistocene–Holocene transition (LPH) approximately 15–10 cal ka BP generated substantial, worldwide shifts in the latitudinal and elevation distributions of plant species and vegetation types. Plant fossil records from the Mojave Desert region of the southwestern USA document the presence of coniferous woodlands during the late Pleistocene in areas now occupied by desert scrub [1–4]. This

palaeobotanical record indicates an upward elevation shift of 600–1000 m in the distributions of many plant species and vegetation zones following the LPH [5–7].

Effects of altered precipitation and temperature regimes on plant survival, growth, and reproduction are implicitly regarded as the direct drivers of such vegetation changes, but multiple factors other than climate can also contribute significantly. The pace at which plant distributions respond to climate change can vary depending on the modes of dispersal of different species. Migration of species with extremely low dispersal ability in some cases lagged millennia behind the arrival of more rapid dispersers after the LPH [8,9]. Refs. [10,11] proposed that “vegetation inertia” involving a lag in the disappearance of some species after climate shifts contributes to periods during which vegetation is composed of a mix of species with various climatic tolerances.

Alterations of soil environments due to increasing climate aridity can drive further changes in vegetation. For example, in arid regions, accumulation of silt- and clay-rich aeolian dust directly beneath a stone pavement [12,13] creates a fine-textured soil horizon that greatly impedes infiltration, thereby greatly reducing the amount of plant-available soil moisture [14,15]. At sites in more arid portions of the Sonoran Desert following the LPH, the development of this soil feature during the course of the Holocene progressively eliminated nearly all perennial vegetation from late Pleistocene fan deposits, creating wide expanses of barren stone pavements [16,17]. Yet, adjacent, younger, mid-late Holocene fan deposits where this soil condition has not developed remain fully vegetated, demonstrating how variable soil hydrologic responses exert an important proximal control on vegetation [18,19]. Soil erosion can also dramatically alter the capacity for storage of plant-effective soil moisture, thereby exerting strong control over vegetation composition, leading to existence of different kinds of vegetation at one locale as a function of contrasting soil conditions [20,21].

This paper focuses on the timing and causes of post-Pleistocene vegetation change on hillslopes at a site in the eastern Mojave Desert. It builds on a geochronological investigation of geomorphic processes, soil formation, and soil erosion at the same site [22]. In the present paper, further information on plant responses to soil conditions, coupled with details of the regional palaeobotanical record, is used to decipher the timing and causes of complex and interrelated responses of vegetation and soils during the Holocene.

2. Study Site and Methods

2.1. Location and Geology

The Nipton Hills study area is 22 km west of Searchlight, Nevada, USA, immediately east of the California-Nevada state boundary (35.46° N, 115.17° W; Figure 1A). The hills are a low-relief terrain of early Proterozoic meta-granitoid, meta-volcanic, and other metamorphic rocks [22,23], separated 4 km from the McCullough Range to the north and 3 km from the New York Mountains to the east and southeast. Multiple linear, subparallel stream drainages through the hills align with the location and spacing of east–west trending faults [23]. The east–west orientation of main axial drainages creates hillslopes on opposite sides of drainages with strongly contrasting, north- and south-aspect exposures (Figure 1B).

Investigations were concentrated within an upper 2 km portion of the southernmost drainage basin (Figure 1A). The west to east elevation gradient of the main axial channel in this portion ranges from 1315 m to 1400 m asl (above sea level) and hillslope relief is approximately 100 m from the channel to hillslope summits. The results presented in this paper are based on information and data collected in the years 2014 through 2021.

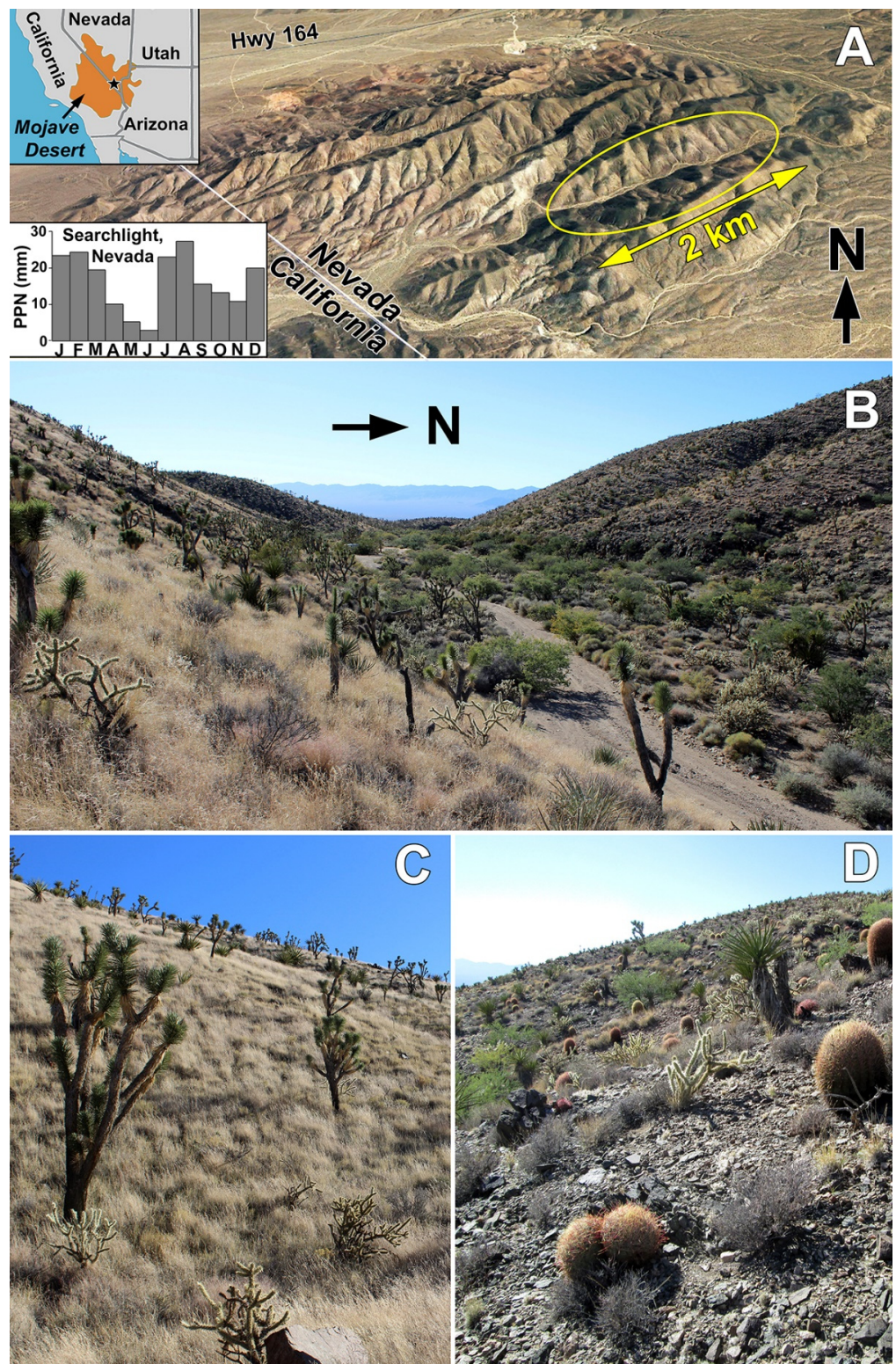


Figure 1. (A). Location of Nipton Hills study area in the Mojave Desert (upper left) and oblique view (Google Earth Pro™) of study area to right. The 2 km long area circled in yellow is the area where investigations of hillslopes were conducted. Lower left inset—average monthly precipitation amounts recorded at Searchlight, Nevada, located 22 km east of Nipton Hills. (B). View westward from central portion of study area, looking downstream along the axial stream drainage separating north- and south-aspect hillslopes. (C,D). Contrasts between perennial grass-dominated vegetation of north aspects and desert scrub vegetation of south aspects.

2.2. Climate

The nearest weather recording station, 22 km to the east and 1080 m asl (US COOP station, Searchlight, Nevada; 1913–2016 recording period) receives 196 mm mean annual precipitation (MAP), with a mean annual temperature of 17.3 °C. The estimated MAP at the study area (computed for 1400 m asl) is ~250 mm, based on a multiple regression relationship between MAP, elevation and longitude for 28 regional recording stations between 200 m and 1600 m elevation [24]. Precipitation is distinctly bimodal, with a pronounced cool-season peak from December through March and a summer monsoonal peak in July through September (Figure 1A). Significant monsoonal input is received throughout the eastern portion of the Mojave Desert, but declines markedly to the west [24,25]. In addition, substantial, but infrequent warm-season precipitation is received in this region via the incursion of tropical Pacific cyclones, principally in September and October [26,27]. The warm-season precipitation inputs contribute to the predominance of perennial C₄ grasses in some portions of this region, including the study area [24].

2.3. Methods

Distinct types of perennial vegetation based on species compositions were identified and mapped. Print copies (1:1000 scale) of color infrared imagery (NAIP imagery from 20 May 2016) of the entire study area were used in the field to locate and draw boundaries around different vegetation units. Ground mapping was conducted in April–May 2018, when foliage of C₄ (warm-season) perennial grasses was dry and straw-colored, permitting areas occupied by grasses to be clearly distinguished from areas of darker, shrub-dominated vegetation. Boundaries of vegetation units were recorded in the field directly on the print imagery and later transferred to polygon shape files in Google Earth Pro™; then used to create the final vegetation map in Esri ArcMap GIS. Total annual insolation modified by topographic shading was modeled for the site using a 3 m grid with Esri ArcMap Area Solar Radiation Tool.

The proportion of the soil surface covered by perennial plant canopies and other types of ground cover was measured at 10 hillslope locations with point-intercept sampling. At locations dominated by a relatively dense cover of perennial grass, measurements were taken using a 1 m-long horizontal pin frame positioned approximately 1 m above the surface, with vertical holes drilled at 10 cm intervals along the frame. Steel pins (6.4 mm diameter) inserted through the regularly spaced holes contacted the underlying surface, and the type of cover contacted by the pin was recorded. The pin frame was moved along linear transects positioned across the slope. For shrub-dominated vegetation, a tape measure was stretched across the sampled area and cover type directly intersecting the tape at 1 m intervals was recorded. For each location sampled, a minimum of 100 point-intercepts were recorded; 250 points were recorded in three locations dominated by perennial grasses. Information on the modern-day geographic and elevational distributions of key plant species, including point maps of individual specimen occurrences, was obtained from online records of mapped, georeferenced herbarium collection records from herbaria located throughout the USA, Mexico, and Canada (<http://swbiodiversity.org/seinet/collections>, accessed on 1 October 2021).

All methods used for soil profile descriptions, laboratory soil analyses, and optically stimulated luminescence (OSL) dating, as well as complete soil profile descriptions, are presented in [22] and supplementary materials of that paper. We follow [28] regarding subdivisions of the Holocene (early Holocene: 11.7–8.2 ka BP; middle Holocene: 8.2–4.2 ka BP; and late Holocene 4.2 ka BP-present). All ages based on published radiocarbon dating are presented as calibrated radiocarbon ages (cal ka BP).

3. Results

3.1. Vegetation Contrasts of Opposite Slope Aspects

Total annual insolation on south-aspect hillslopes is approximately 70% greater than that received on north aspects (1.6×10^6 vs. 9.2×10^5 W/m²; Figure 2A,B), and the opposite aspects contrast strongly with respect to vegetation. Two perennial C₄ grass species, *Hilaria jamesii* (galleta) and *Bouteloua eriopoda* (black grama) provide relatively dense ground cover across most north-aspect hillslopes (Figures 1C and 2C), and those perennial grasses together with other plants cover approximately 60–70% of the soil surface (Table 1: North aspect, thick colluvial mantle). In addition to the areas dominated by one or both of these perennial grass species, some north-aspect hillslopes in the upper portion of the basin are occupied by a mixture of the two grasses and shrubs (*Menodora spinescens* or *Coleogyne ramosissima*; Figure 2C).

Table 1. Perennial plant canopy cover on various soil environments of north-versus south-aspect hillslopes. Data represent point-intercept estimates of percent of the ground surface covered by each category.

Sample Sites:	North Aspect				South Aspect				
	Thick Colluvial Mantle			Thin Colluvial Mantle		Older Colluvial Remnant		Distal Fan Apron	
	N1	N2	N3	S1	S2	S3	S4	S5	S6
Perennial grass species									
<i>Hilaria jamesii</i>	67	41	54					42	
<i>Bouteloua eriopoda</i>		15	16			3			3
<i>Hilaria rigida</i>						43	45		48
<i>Muhlenbergia porteri</i>		2							
<i>Tridens muticus</i>					3				
<i>Dasyochloa pulchella</i>				1	1				
Total % cover (perennial grasses)	67	58	70	1	4	46	45	42	51
Shrub species									
<i>Menodora spinescens</i>	+		+						
<i>Ephedra nevadensis</i>	2	3	+	1		4		4	
<i>Eriogonum fasciculatum</i>				9	6				
<i>Encelia virginensis</i>				1	7				
<i>Krameria erecta</i>				2	3	4		4	
<i>Acacia [= Senegalia] greggii</i>				1	1				
<i>Larrea tridentata</i>					2				
<i>Aloysia wrightii</i>					2		+		+
<i>Adenophyllum cooperi</i>				4					
<i>Coleogyne ramosissima</i>				2					
Total % cover (shrubs)	2	3	<1	20	21	8	<1	8	<1
Succulent species									
<i>Cylindropuntia ramosissima</i>			+	9	+	+	+	+	+
<i>Ferocactus cylindraceus</i>				1	1	+	+	+	+
<i>Yucca brevifolia</i> var. <i>jaegeriana</i>	+	+	+						
<i>Yucca schidigera</i>				2	2	+	+	+	+
<i>Yucca baccata</i>			+	1					
Total % cover (succulents)	<1	<1	<1	13	3	<1	<1	<1	<1
Total % Perennial Plant Cover	69	61	70	34	28	54	45	50	51

+ indicates present at site but <1% cover as measured by point-intercept sampling.

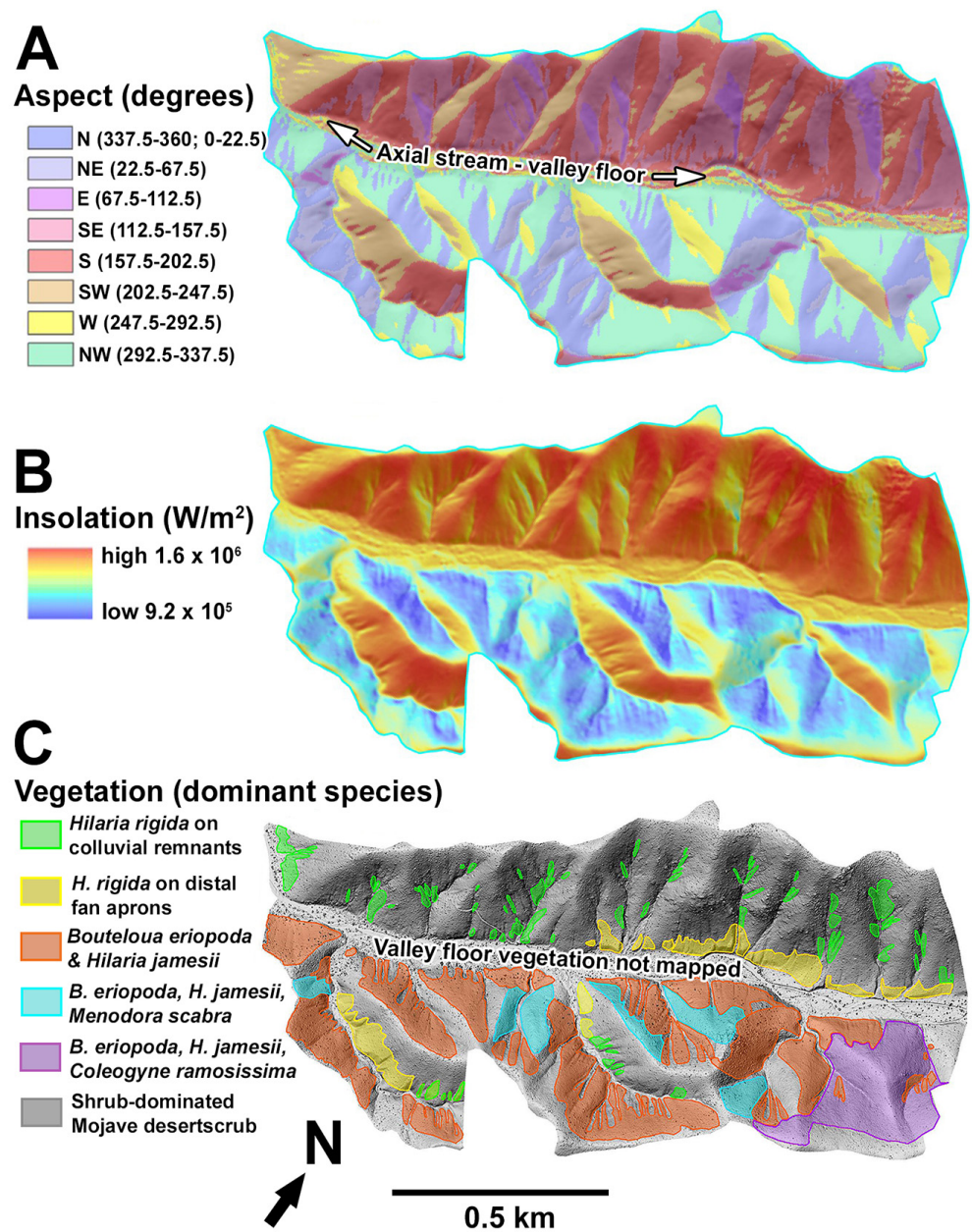


Figure 2. (A). Distribution of hillslope aspects on opposite sides of the axial stream. Southeast and south aspects predominate on hillslopes on the north side of the axial stream; north, northeast, and northwest aspect predominate to the south of the axial stream. The southern tributary basins to the main axial stream curve towards the east, producing significant aspect contrasts (northern vs. southern) in these tributary basins. (B). Total annual insolation, modified by topographic shading of hillslopes. (C). Mapped vegetation within the study area. The green-shaded areas are the patches dominated by the perennial grass *Hilaria rigida* on colluvial remnants on south aspects. These are contained within a larger matrix (gray) of shrub-dominated desert scrub vegetation.

Desert shrubs and succulents occupy most of the south-aspect hillslopes (Figure 1D), where they cover only a third or less of the soil surface (Table 1: South aspect, thin colluvium). However, distinct patches dominated by a third perennial C₄ grass species, *Hilaria rigida* (big galleta), occur within this matrix of sparse desert scrub (Figures 2C and 3B). Within those grass-dominated patches, perennial vegetation covers only approximately half of the soil surface in (Table 1: South-aspect, older colluvial remnant). The grass-covered patches are typically clustered within broad topographic concavities of tributary basins to the main axial stream (Figure 2C). Individual patches are typically elongated, and bounding first-order channels are cut to bedrock and depths of up to 1.5 m (Figure 3B).

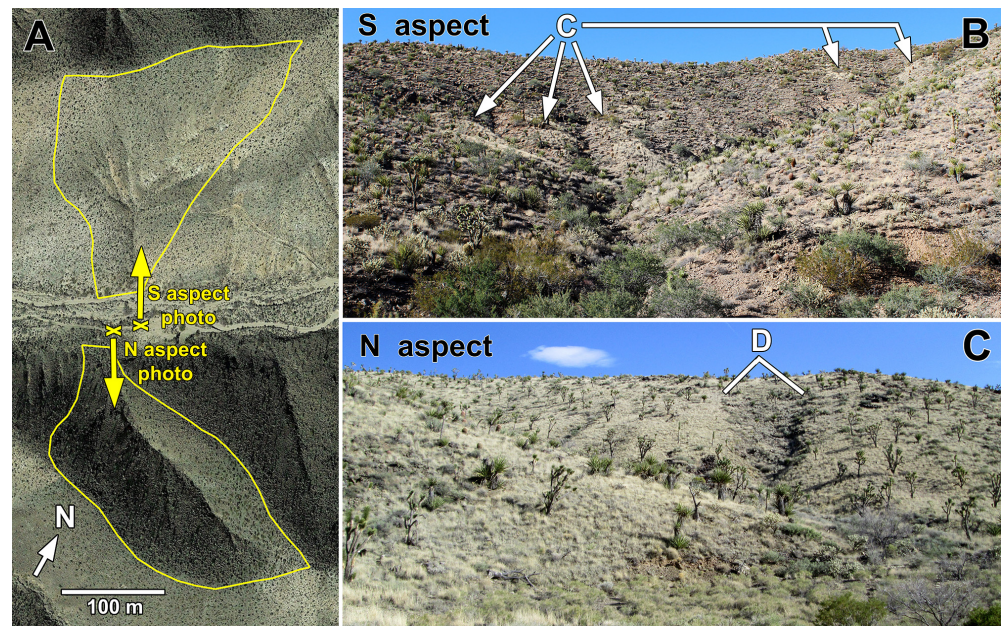


Figure 3. (A). Vertical aerial view (Google Earth Pro™) of a pair of similar-sized tributary basins on north and south sides of main axial drainage (2.9 ha & 2.7 ha, respectively), showing camera locations and directions of the ground-level photographs on the right. (B). Ground-level view of south aspect showing colluvial remnants (C) covered with light-colored *Hilaria rigida*. Darker-colored, shrub-dominated desert scrub vegetation occupies intervening areas. (C). Ground-level view of north aspect showing extensive perennial grass cover occupying deep soils developed in a thick colluvial mantle. The debris-flow scar (D) exposes underlying bedrock; the apex of the debris fan is in the lower right hand corner. The light-colored areas dominated by perennial grass contrast with the darker debris flow scar containing exposed bedrock (dark metabasalt) and sparse cover of woody plants. Planar foliation of the exposed metabasalt on the floor of the debris flow scar is nearly parallel to the slope inclination, likely contributing to slope instability at this particular location.

Less inclined (12% slope inclination vs. 25% on adjacent, steeper hillslopes), broad and thick colluvial/alluvial fan aprons at the base of south-aspect hillslopes border the main axial stream and the larger tributary basins (Figure 4), and are also occupied by *H. rigida*, with occasional *H. jamesii* and *B. eriopoda*, and a total canopy cover of approximately 50% (Table 1: South aspect, distal fan apron). Extensive, thick fan aprons such as these are absent along the base of north- aspect hillslopes.

3.2. Hillslope Soils

Detailed information on soils of the site, including OSL ages that provide constraint on the timing of soil formation and erosion, and complete soil profile descriptions is presented in [22]. Portions of the following in Sections 3.2.1–3.2.3 summarize those results in order to provide the necessary, integrated context for understanding vegetation responses to soil conditions and the timing of palaeoecological changes.



Figure 4. Broad fan aprons along base of south aspect hillslope, with the axial ephemeral stream positioned next to the trimmed distal portion of the apron. An unpaved road extends from the bottom center of view to left center. The light-colored vegetation of the fan aprons is dominated by *Hilaria rigida*. The darker, upper hillslopes with thin, transient colluvial mantles and bedrock exposures are occupied by shrub-dominated desert scrub.

3.2.1. Soil Characteristics

The dense, perennial grass-dominated vegetation on north-aspect hillslopes occurs exclusively on relatively thick (0.3–1.5 m) soils that have developed within colluvium composed of coarse gravel to larger, subangular and angular clasts. These soils contain Bw and Btk horizons with silt loam textures (silt contents >50%), and low rock plus gravel content (Figure 5). In contrast, south-aspect hillslopes occupied by sparse, shrub-dominated desert scrub lack well-developed soils, and the substrate consists of a thin mantle of gravelly regolith up to ~15 cm thick over bedrock, with patches of bedrock exposed on the surface. The thin soils are weakly developed, consisting of very gravelly, loamy sand A horizons and gravelly, loamy sand Ck horizons over fractured bedrock. Exposed bedrock accounts for 17% of the total area of south-aspect hillslopes, but only 10% of north-aspect hillslopes.

The small areas dominated by the grass *H. rigida* on south aspects (Figures 3B and 6) occur exclusively on scattered patches of thick, moderately well-developed soils that have formed in coarse gravel-to cobble-rich colluvium (termed colluvial remnants hereafter). The soils of those remnants are similar in thickness and horizon development to those on north-aspect hillslopes, with slight reddening and Btk horizons with silt-loam textures and low rock plus gravel content (Figure 6). These patches represent partially truncated, eroded remnants of what at one time was a more extensive, thick colluvial mantle containing a well-developed soil. Only 4% of the total area of south-aspect hillslopes is covered by these colluvial remnants with perennial grass-dominated vegetation compared to 79% of north-aspect hillslopes (Figure 2C).

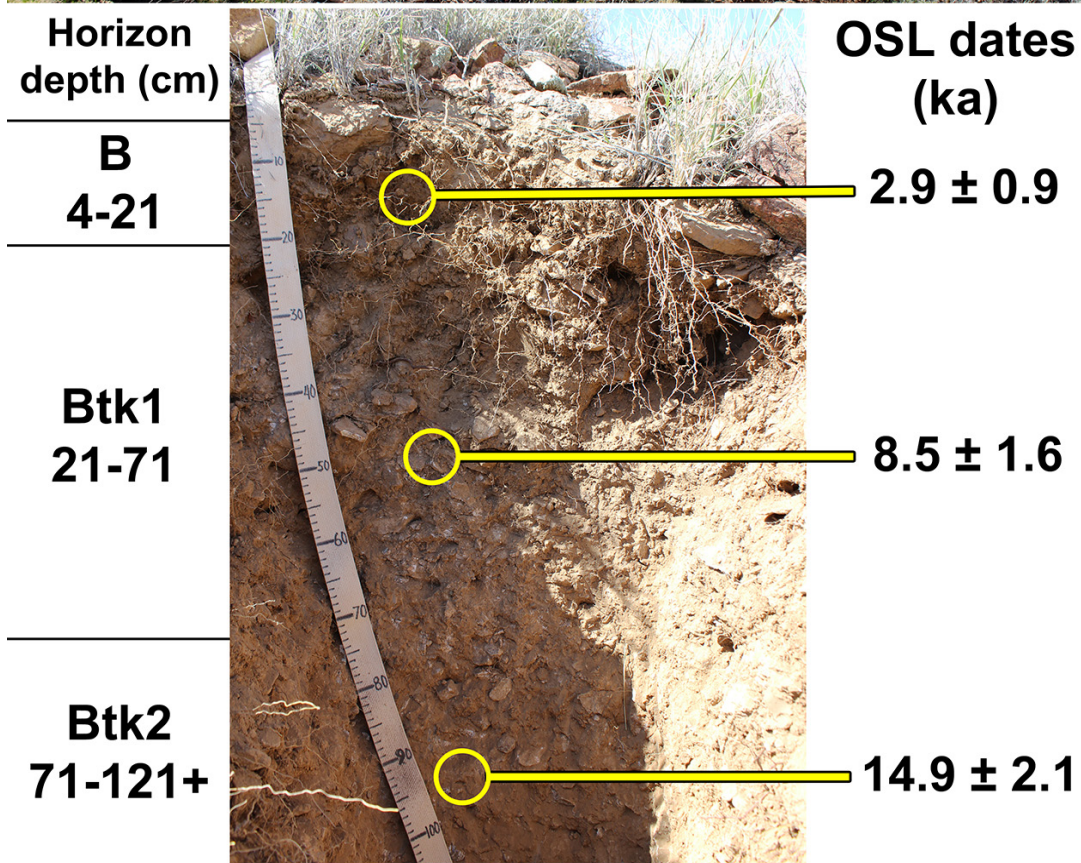


Figure 5. (Top). Location of soil profile 11-Apr-15-1 on north aspect. Perennial grass vegetation consists primarily of *Hilaria jamesii* with lesser amounts of *Bouteloua eriopoda*. (Lower). Soil profile showing locations of three OSL samples and associated ages. Length of rule on left is 103 cm. Note abundance of diffuse, fibrous roots of *H. jamesii* within the upper 40 cm of the soil. Image of soil profile with OSL dates modified from Figure 4A in [22]. Photograph on 11 April 2015.

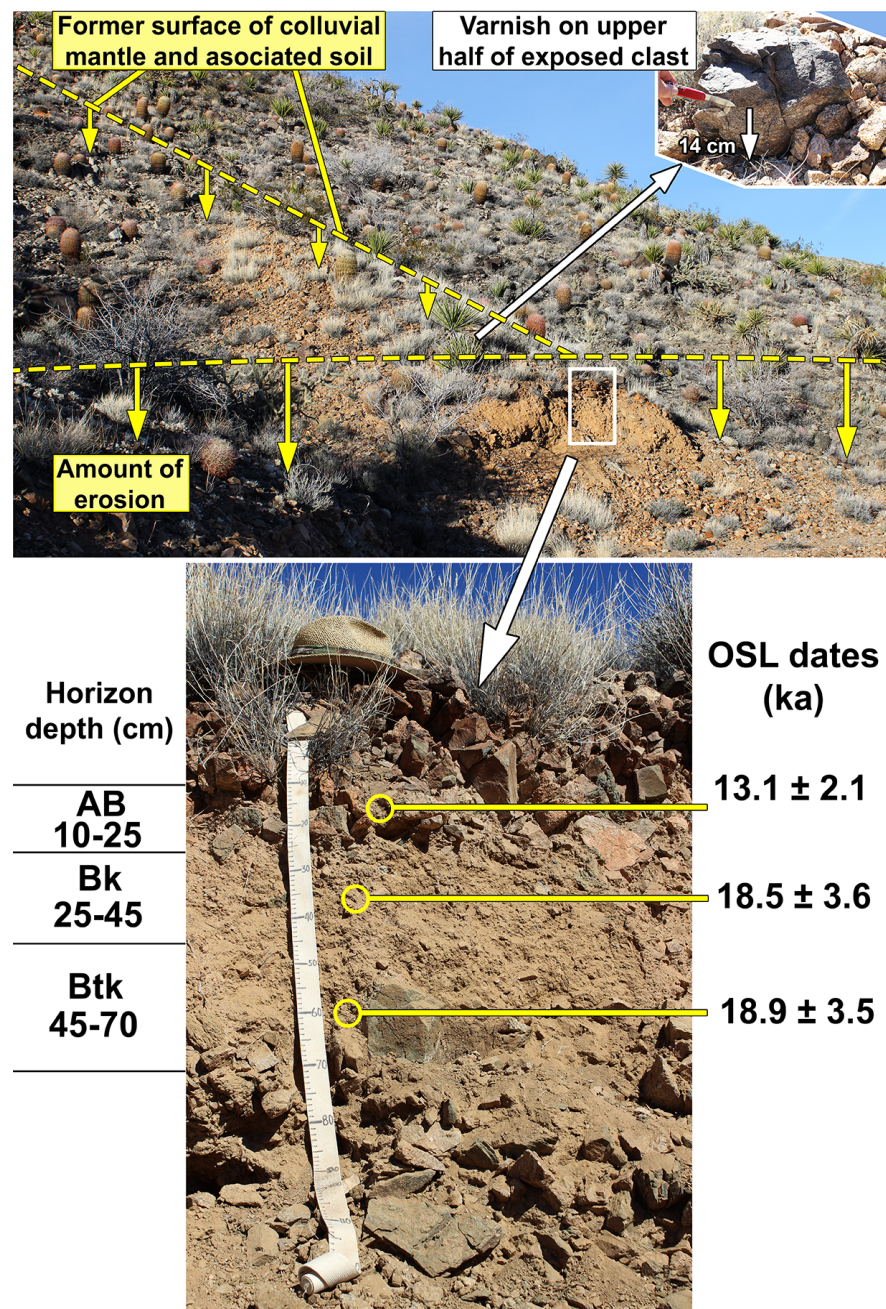


Figure 6. (Top). Cross-section through isolated colluvial remnant on south aspect. Dashed yellow lines suggest the surface configuration of the original colluvial mantle; yellow vertical arrows indicate extent of subsequent erosion. Inset on upper right shows the large clast on the center surface of the remnant with varnish on upper most surface and evidence for the erosional removal of 14 cm depth of materials at that location. Light-colored plants on the colluvial remnant surface are *Hilaria rigida*. Several *Yucca schidigera* and a barrel cactus *Ferocactus cylindraceus* are also present. The surrounding area lacking a thick colluvial mantle and soil is dominated by shrubs (*Eriogonum fasciculatum*), occasional *Larrea tridentata* and *Acacia greggii*, cacti and yuccas. The white rectangle indicates the location of soil profile shown below. **(Lower).** Soil profile 16-Dec-14-1 from the exposed face of the colluvial remnant shown above and locations of OSL samples and associated dates. Note the nearly clast-free Bwk and upper half of the Btk horizons. Roots of *H. rigida* are concentrated in the upper 30 cm of the soil. Image of soil profile with OSL dates modified from Figure 4A in [22]. Photographs taken 16 December 2014.

Soils of the wide fan aprons at the base of south-aspect hillslopes are considerably thicker (>2.5 m) than those that have formed in the colluvial deposits of steeper hillslopes on either north- or south-aspects (see Table S1 in [22]). Those thicker soils have well-developed Bt horizons with silt-loam texture and exhibit more advanced profile development than those formed in steeper hillslope colluvial deposits (e.g., Stage II vs. Stage I calcium carbonate accumulation, [29]).

3.2.2. Formation and Age of Hillslope Soils

The fine-textured fractions of the silt-rich horizons in the soils on north-aspect hillslopes (Figure 5) and the colluvial remnants of the south-aspect (Figure 6) are largely derived from the input and accumulation of aeolian sediments, as is the general case for soils throughout this arid-to semi-arid region [12,30–34]. Deposits of coarse gravelly to stony colluvium function as excellent dust traps [35,36], and there are plentiful, nearby sources of aeolian sediments. The study area is 15 km east and downwind of the nearly vegetation-free, 42 km² Ivanpah Playa. Margins of playas, vegetation-free channels of ephemeral streams, and distal alluvial fans like those immediately surrounding Ivanpah Playa are among the largest sources of aeolian sediment in the region [37–39]. Prevailing westerly winds have transported and deposited aeolian sediments from that area, forming broad dune deposits that extend up to 7 km east of the margin of Ivanpah Playa [23] (Figure 7). Finer aeolian sediments (very fine sand, silts and clays) can be transported considerably further. Direct evidence for the aeolian origin of fine sediments (63–150 μm) within soils at the site includes elemental compositions and surface morphology of sediment granules, and strong luminescence responses of quartz granules of that size range used for OSL dating [22]. OSL dating of those fine sediments provides information on the length of time that has elapsed since the grains were last exposed to light during aeolian transport.

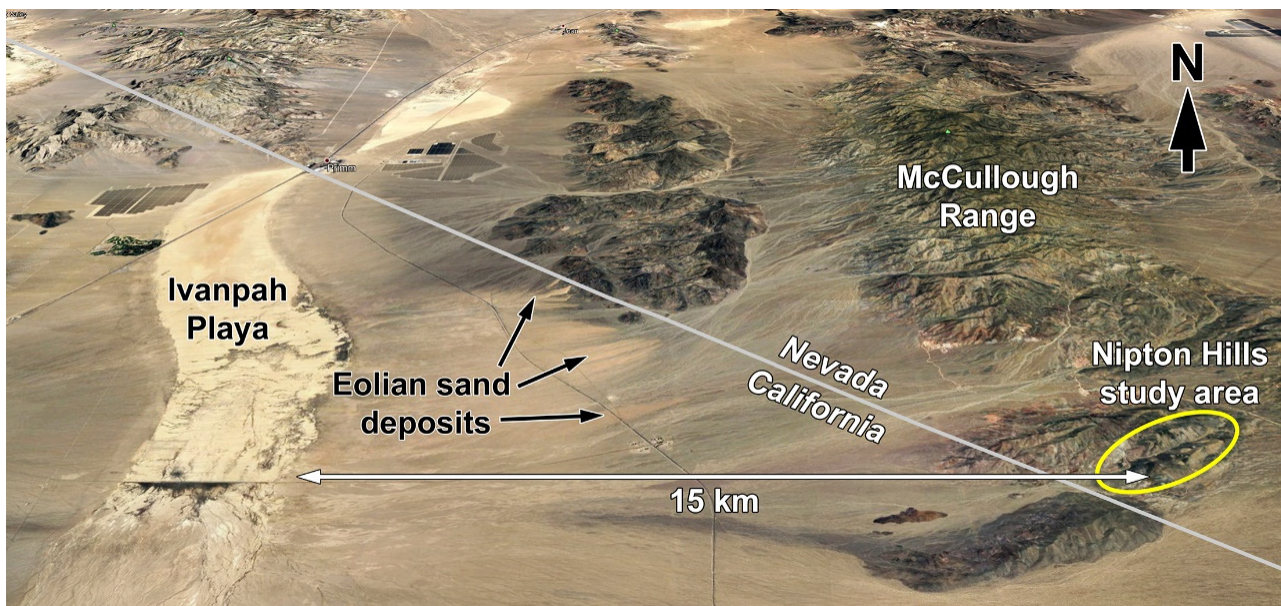


Figure 7. Location of Ivanpah Playa in relation to the Nipton Hills study area. The playa margin and distal alluvial fans are major sources of aeolian dust transported east by prevailing winds.

OSL ages estimates for the north-aspect site and the south-aspect colluvial remnant [22] are similar in that the oldest sediments are those from deeper horizons and date to the late Pleistocene (14.9 ka and 18.9 ka for north and south aspects, respectively: Figures 5 and 6). The older ages at greater depths are interpreted as the result of the ease at which fine sediments were initially translocated downward within large voids and passageways within coarse, gravelly colluvium. Eventually, deep translocation likely became increasingly obstructed as fine materials filled voids, resulting in the subsequent accumulation of younger aeolian sediments at progressively shallower depths. These OSL ages, as well as soil profile characteristics [22] are similar to those of soils formed in latest Pleistocene alluvial fan deposits at another nearby location in the Mojave Desert [40].

OSL ages from north and south aspects differ in that sediment ages from shallower depths are significantly younger in the north-aspect profile than in the south aspect. Sediments from the Btk1 and B horizons of the north aspect have early Holocene (8.5 ka) and late Holocene (2.9 ka) ages (Figure 5). In contrast, sediment ages from all depths in the south-aspect profile date to the late Pleistocene, ~13–19 ka (Figure 6). This contrast indicates that accumulation and incorporation of aeolian sediments apparently has been an ongoing process from the late Pleistocene and throughout the Holocene, in soils of the north-aspect where the dense perennial grass serves as an effective dust trap [41]. However, this continual accumulation has not occurred on the more sparsely vegetated colluvial remnants of the south-aspect.

3.2.3. Timing of Major Episode of Hillslope Erosion

Material transported and deposited downstream by the main axial ephemeral stream provides a record of the magnitude and timing of a major episode of hillslope erosion during the Holocene [22]. A prominent alluvial fill terrace, the surface of which is approximately 1.5 m above the current stream channel, is present up to 2.5 km downstream from the hillslope study area (Figure 8A). Beyond 2.5 km downstream, local relief of different-aged alluvial surfaces diminishes as alluvial deposits broaden into a fan complex, integrating sediments derived from multiple drainage basins. A distinguishing characteristic of the terrace remnants is the presence of large, circular or elliptical clones of the shrub *Larrea tridentata* (creosotebush) with basal diameters up to 3.0 m (Figure 8B,C). Creosotebush clones of this size require at least a few millennia to grow to such diameters [42,43]. The terrace is composed of coarse gravel- to cobble-rich alluvium within which a weakly developed soil has formed (Table S1 in [22]). The degree of horizon development (Bk horizons, stage I carbonate accumulation) is similar to those of dated mid-Holocene fan deposits described in the region [40]. The presence of prominent silt caps on tops of clasts within the AB and Bk horizons provides direct evidence of the downward translocation and accumulation of aeolian dust. OSL ages of fine sediment within the Bk1 and Bk2 horizons were 3.2 ± 0.6 ka and 3.5 ± 0.4 ka, respectively [22]. These ages of aeolian sediments post-date to some degree the actual timing of somewhat earlier deposition of the coarse gravelly to cobbly alluvium. Consequently, original alluviation likely occurred around the time of the middle-late Holocene transition (4.2 ka BP) or shortly thereafter. The height of the mid-Holocene terrace and broad area over which it occurs indicated a considerable volume of materials eroded from hillslopes and evacuated from the drainage basin (Figure 8A). However, most of those sediments had to be derived from the erosion of soils from south-aspect hillslopes formed during the late Pleistocene, because comparable soils that support denser vegetation on north aspects remained largely intact through the LPH and the entire duration of the Holocene.

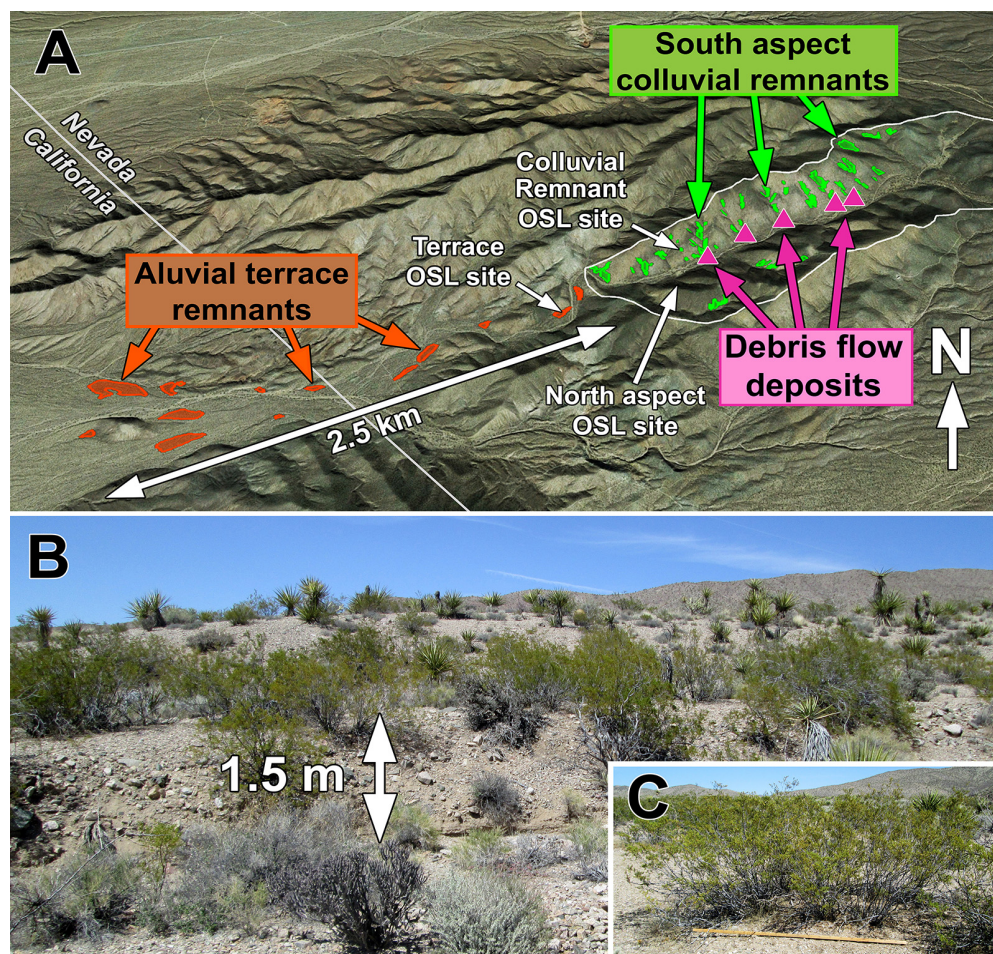


Figure 8. (A). Distributions of colluvial remnants on south aspect hillslopes (green) and alluvial terrace remnants (orange) downstream from hillslope study area. Magenta triangles indicate the location of debris flow deposits. White boundary around hillslope area designates the drainage divides. (B). View of the 1.5 m-high terrace tread. The remnant shown is the one indicated by the central orange arrow in A. The green shrubs are creosotebush, *Larrea tridentata*. (C). Large creosotebush (*Larrea tridentata*) clone with a ring-shaped base over 2 m in maximum diameter on a terrace remnant. The horizontal rod in foreground is 2 m long.

The prominent fan aprons along the base of south-aspect hillslopes are deeply incised (up to 4 m) by the axial channel and tributary channels and grade to a considerably higher, former valley floor (Figure 4). Older debris flow deposits are emplaced on top of the wide fan apron and contain boulders up to 1 m diameter (Figure 9). Upper surfaces of those boulders are coated with dark, continuous varnish and lower (subaerial) surfaces are very strongly reddened (5YR hues), features that indicate an older age than the LPH. Characteristic of soil profiles from the fan aprons, particularly a more advanced stage II carbonate horizon development, also indicate an age greater than that of the late Pleistocene colluvial deposits on steeper portions of hillslopes. Additionally, younger debris flow deposits are present on narrow terraces along the tributary channels, inset below the uppermost fan apron surface (Figure 9). The multiple deposits indicate a long history of debris flows on south-aspect hillslopes during the late Quaternary which would have contributed substantial amounts of material to the axial valley floor. Although several debris flow scars are present on north-aspect hillslopes, those features are small in comparison to debris flow deposits at the base of south-aspect hillslopes (e.g., Figure 3C), indicating a lesser magnitude of materials removed by mass wasting during the late Quaternary in those more densely vegetated settings.

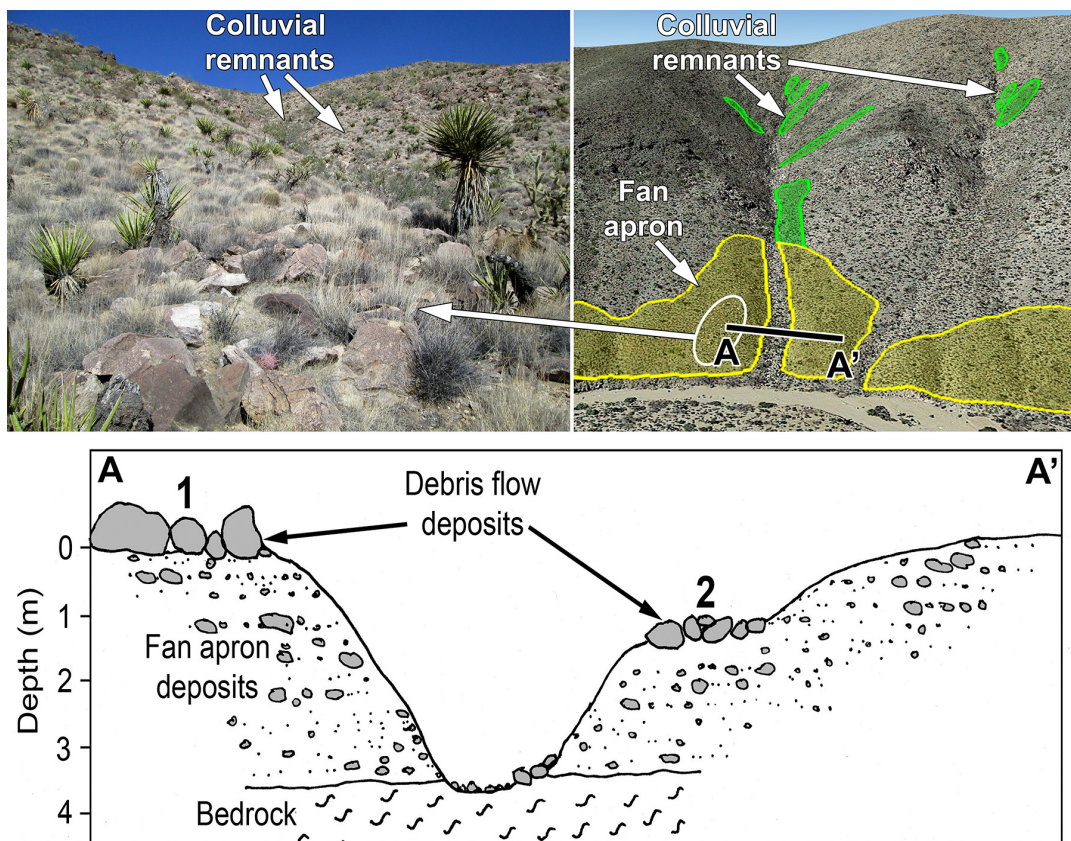


Figure 9. (Upper left) Debris flow lobe containing boulders up to 1 m diameter emplaced on top of fan apron surface. Weathering-resistant boulder surfaces are darkly varnished (lower left), indicating a late Pleistocene deposit. (Upper right) Low-angle, oblique aerial view (Google Earth Pro™) showing position of boulders in debris flow lobe (white circled area) emplaced on top of fan apron surface (yellow). The line A–A' is the location of the cross section diagrammed below. Multiple, narrow colluvial remnants (mapped in green) remain in upper, more steeply inclined portions of the hillslope. (Lower panel) Cross-section across channel of tributary basin showing position of different-aged debris flow deposits positioned on top of the uppermost fan apron surface (1) and younger, terrace-like inset surface (2). An additional set of more recent debris flow deposits located just above the channel floor was identified at some of the debris flow locations mapped in Figure 8.

3.2.4. Extent of Hillslope Soil Erosion on South Aspects

In addition to erosion along lateral margins of colluvial remnants on the south aspect, there has been a substantial vertical extent of soil loss from those remnant surfaces. For example, in the center of the colluvial remnant of the south-aspect OSL sample site, an extremely large clast (40 cm diameter), firmly anchored within the underlying substrate, possesses thin coatings of dark rock varnish on the upper portions (Figure 6). The varnish coating has a sharp lower boundary 14 cm above the surrounding soil surface. The lower surface exhibits pedogenic iron oxide reddening (termed “ventral varnish” [44]). Additionally, in one of the colluvial remnants pictured in Figure 3B, the uppermost surfaces of a large, deeply anchored surface clast are varnish-coated, but with a sharp, linear boundary parallel to and 30 cm above the current surface, and pedogenic iron oxide reddening of the lower portion. These observations indicate that erosion has lowered the soil surfaces of those remnants below their original levels (Figure 6). In contrast, surfaces of larger exposed clasts in densely grassed areas of north-aspect hillslopes are typically entirely covered with dark “dorsal” varnish, or occasionally with lichens to the soil surface, indicating very little erosion.

Differences in color and texture of A horizons also reflect the erosion of materials from the surfaces of south-aspect colluvial remnants, but the lack of comparable erosion on the north aspect. The A1 horizon of the north aspect profile (Table S1 in [22]) is a dark brown (10YR 3/3) loam, reflecting the accumulation and retention of organic matter in a persistent horizon. In contrast, the A horizon of the south aspect profile lacks this darkening and is a yellowish-brown (10YR 5/4) silty loam, more similar in Munsell color value and texture to underlying B horizons, reflecting the lack of accumulation of organic materials and erosional truncation. The substantially greater surface erosion of south- aspect colluvial remnants further explains the lack of younger aeolian sediments in upper soil horizons as described in the last section. In addition to the limited dust-trapping ability of the sparser vegetation, new aeolian sediments deposited on the surface are probably regularly removed by overland flow.

3.2.5. Effective Ground Cover and Soil Erosion

The soils developed in colluvial deposits on north and south aspects differ markedly in effective ground cover provided by perennial vegetation and plant litter. On north aspects, basal area of perennial grass plants (the tight, central clustering of stems at the base of a plant) together with plant litter on the soil surface beneath canopies of perennial grass covers nearly half (11.6% plus 36%) of the ground surface (Figure 10). These two types of cover provide the most effective protection from erosion. In contrast, where *H. rigida* predominates on soils of colluvial remnants on south-aspect hillslopes, perennial grass basal area and plant litter beneath grass canopies covers only about a fifth (9.7% plus 11.5%) of the ground surface. Those areas on the south aspect have three times the proportion of exposed, fine-grained soil beneath plant canopies (10.3%) than do north aspects (3.2%) (Figure 10).

The reduced effective ground cover and direct exposure of fine-grained soils to erosion on south aspects is due to a combination of both reduced total canopy cover as well as above-ground architecture of *H. rigida*. Individual plants of this coarse bunch grass are widely separated and have a relatively small basal area with stiff, upright culms that do not closely cover the soil surface (Figure 10). In contrast, the denser growth of *H. jamesii* and *B. eriopoda* on north aspects generates a compact, sod-like cover through lateral spread by basal tillering (*H. jamesii*) or stoloniferous reproduction (*B. eriopoda*).

3.3. Root Systems, the Distribution of Soil Moisture, and Soil Moisture Extraction by Plants

Fundamentally different architectures of root systems of perennial grasses versus woody shrubs enable the two groups of plants to occupy soil environments that contrast strongly in the spatial distribution and temporal duration of soil moisture. The grasses possess relatively shallow, diffuse fibrous root systems that densely occupy fine-grained soil horizons within a half-meter or less of the surface (Figures 5 and 11A). The fine-textured B horizons developed in late Pleistocene colluvium have high water-holding capacities and consequently, relatively little moisture moves to greater depths. The diffuse fibrous, but relatively shallow root systems of perennial grasses rapidly extract moisture retained in these fine-grained B horizons during a relatively brief growing season. When those moisture reserves are seasonally depleted, the perennial grasses become dormant until favorable growing conditions recur. In summary, plant-available moisture within the soils developed in older colluvium is characterized by a relatively shallow, spatially homogeneous, but seasonally variable distribution that is efficiently and rapidly exploited by the diffuse fibrous root systems of perennial grasses [24,45].

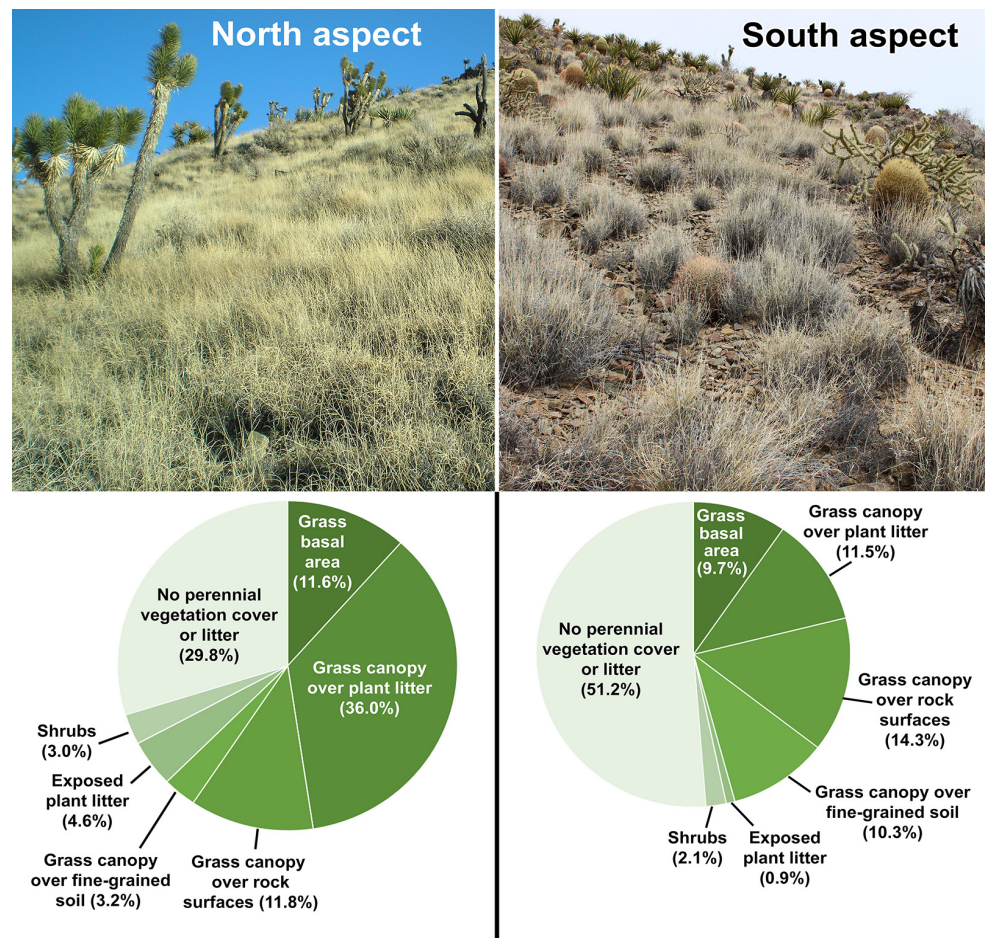


Figure 10. (Top panels). Close-up photographs showing contrast in vegetation cover provided by perennial grasses on the thick soils formed in colluvium on north and south aspect hillslopes. *Hilaria jamesii* and *Bouteloua eriopoda* provide dense cover on the north; the upright, separated individual anopies of *H. rigida* on the south aspect provide substantially less effective cover. (Lower panels). Details in the amount of various kind of effective ground cover on north versus south aspect hillslopes.

In contrast, woody shrubs that predominate in areas of very thin soils over fractured bedrock, mostly on south aspects, have woody taproots that penetrate bedrock fractures and joints. The thin, gravelly soils at the surface have far less moisture-holding capacity, and water percolates through fractures and joints in the underlying bedrock, where it is stored at greater depth. The shallow, diffuse fibrous root systems of grasses cannot access those moisture resources, but the deep taproots of woody plants are able to do so [46]. Woody taproots of *Eriogonum fasciculatus* extend to depths of a meter or more in bedrock fractures and joints, and the larger shrub *Acacia greggii* can have roots that extend even further to depths of several meters (Figure 11B,C). Moisture infiltrating and stored at such depths in bedrock joints and fractures is retained for longer durations than moisture stored at relatively shallow depths [47–49]. The contrast between rooting patterns and water exploitation strategies of shallow-rooted perennial grasses versus deep-rooted woody plants has been widely documented for other arid and semi-arid environments in the American Southwest [45] and worldwide [50,51].

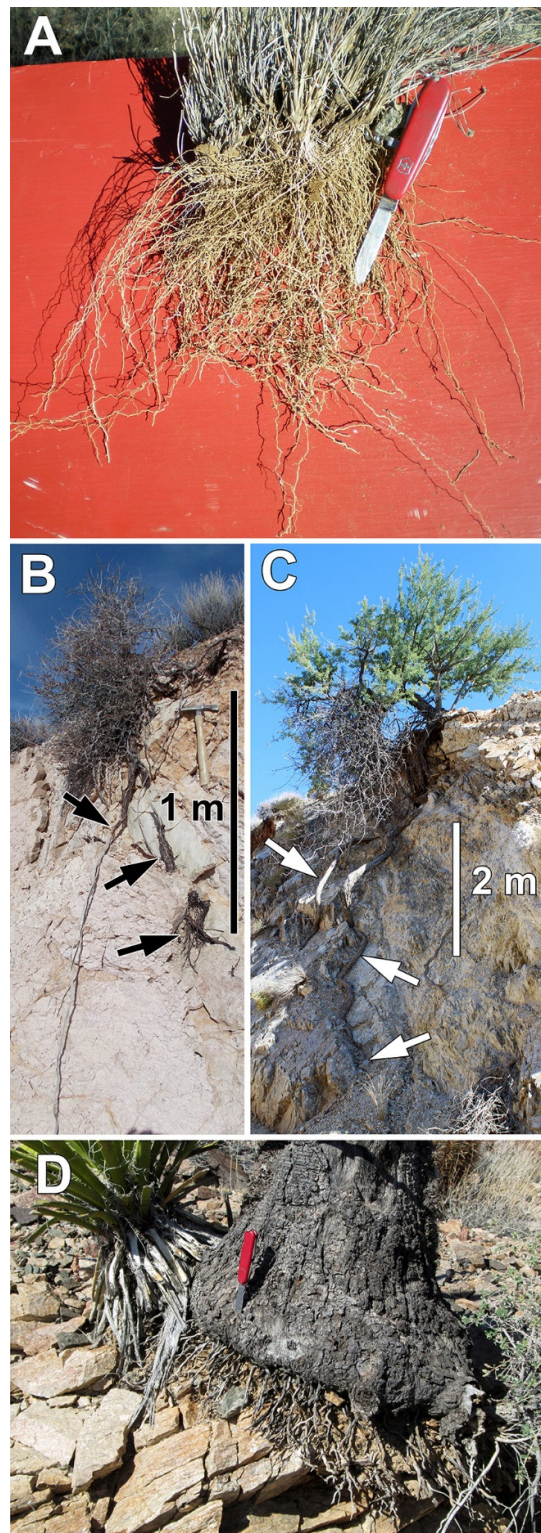


Figure 11. (A) Diffuse, fibrous root system of *Bouteloua eriopoda*. Total length of knife, including blade is 16 cm. (B) Taproots of *Eriogonum fasciculatus* exposed in excavated cut, extending to depths exceeding 1 m in bedrock fractures and joints. (C) Multiple taproots of *Acacia greggii*, one extending to over 6 m depth, exposed in an excavated cut. (D) Shallow root system of stem succulent plant, *Yucca schidigera*, exposed in an excavated cut. The roots originally occupied a thin soil mantle less than 15 cm deep over fractured bedrock.

A third group consists of succulent plants that store water internally. The shallow roots of these plants rapidly extract soil moisture when briefly available, store this moisture in fleshy tissues, and subsequently draw on those stores during dry periods when soil moisture is no longer available. Succulent plants that are abundant on the thin soils of south aspects include *Yucca schidigera*, *Cylindropuntia acanthocarpa*, and *Ferocactus cylindraceus* (Table 1 and Figure 11D). These species have shallow root systems capable of extracting moisture when it is briefly available in the thin, gravelly soils covering fractured bedrock or from shallow depths of the soils developed in the older, thicker colluvial deposits.

3.4. Modern Distributions of Predominant Perennial Grasses in Relation to Climate

The three predominant perennial grasses that occupy hillslopes at the Nipton Hills differ in their present-day distributions along aridity gradients controlled by elevation. *Hilaria rigida*, found only on the more xeric south aspects, occurs in far more arid environments than either *H. jamesii* or *B. eriopoda*. Its distribution extends to areas receiving 80 mm or less average annual precipitation (e.g., below sea level in the Salton Sink, California and to near sea level along the Gulf of California in Sonora and Baja California Norte, Mexico). In the eastern Mojave Desert region, *H. rigida* ranges from the lowermost elevations near the Colorado River (~150 m asl), up to approximately 1600 m asl, depending on aspect and soil conditions, but is most common below 1400 m asl [24].

In contrast, the principal geographic ranges of *B. eriopoda* and *H. jamesii* include semi-arid grasslands to the east and northeast that receive considerably greater precipitation. *Bouteloua eriopoda* occurs from central Texas westward through New Mexico and Arizona, and southward into north-central Mexico, where average annual precipitation in some places exceeds 350 mm. *Hilaria jamesii* occurs widely throughout the Great Basin region in Nevada, the Colorado Plateau and across the northern half of New Mexico and southeastern Colorado to the western-most part of the Texas panhandle. In the eastern Mojave Desert region of southern Nevada and adjacent California, *B. eriopoda* and *H. jamesii* typically occur between 1300–1700 m asl [24].

Another grama grass species, *Bouteloua gracilis* (blue grama), also occurs in the eastern Mojave Desert region, but generally at higher elevations than the species described above. At the Nipton Hills site, three plants of *B. gracilis* growing in a cluster were discovered on a north- aspect hillslope (35.45178° N, 115.16495° W, 1400 m asl), and probably represent a relict of a far more common occurrence at the site during the late Pleistocene. Ref. [52] reported *B. gracilis* from an ~11 cal ka BP woodrat midden collected at ~1280 m asl in Joshua Tree National Park, 180 km SSW of the Nipton Hills. The current distribution of *B. gracilis* in areas surrounding the study area indicates a contraction to higher elevations in the Mojave Desert region from a considerably wider distribution during the late Pleistocene. Today *B. gracilis* commonly occurs at elevations of 1500 m to over 2000 m asl in mountains and highlands surrounding the study area (New York Mountains, McCullough Range, Clark Mountains, Mescal Range, and Cima Dome), typically in association with pinyon-juniper woodlands [24]. It is also widely distributed throughout the San Bernardino Mountains, 200 km southwest of the study area at elevations ranging from 1670 m asl, where it occurs in juniper woodlands, to over 2770 m asl where it is found in pinyon-juniper woodlands and forests of *Pinus jeffreyi* (Jeffrey pine). It also occurs above 1700 m asl throughout the Spring Range and Sheep Range, 100 and 130 km north of the study area, and further north into the Great Basin of central and eastern Nevada to approximately 39° N latitude (mapped, georeferenced herbarium collection records from <http://swbiodiversity.org/seinet/collections>; accessed on 1 October 2021).

4. Discussion

4.1. Reconstruction of Late Quaternary Vegetation Changes

4.1.1. Late Pleistocene Vegetation at Nipton Hills

Plant macrofossil evidence for the Mojave Desert region obtained from ancient woodrat middens indicates that vegetation at the Nipton Hills study area during the late Pleistocene would have included *Pinus monophylla* (single-leaf pinyon pine) and *Juniperus osteosperma* (Utah juniper). Although midden records have not yet been reported for the immediate vicinity and elevation of Nipton Hills, records from other Mojave Desert localities at comparable elevations and latitudes provide relevant information. At sites located 125–143 km directly west of Nipton Hills (35.35° to 35.43° N) and similar elevations (1220–1320 m), *P. monophylla* and *J. osteosperma* were present in each of five middens ranging from 11.2–27.9 cal ka BP [53]. However, four middens from the same locales dated 7.8–8.8 cal ka BP lacked both. At another site located 35 km west-southwest of Nipton Hills (35.33° N, 115.55° W) and 1490 m elevation, two middens with ages of 4.9 and 5.6 cal ka BP also lacked pinyon and juniper.

Records from fossil woodrat middens for sites throughout the Mojave Desert indicate an upward elevation shift of 600–1000 m asl from the late Pleistocene to the present in the lowermost occurrences of pinyon pine and juniper [5,6]. Vegetation at higher elevations in the nearby McCullough Range provides a reasonable analog of the type of vegetation cover that may have existed at Nipton Hills during the late Pleistocene. The southern half of the McCullough Range consists of the same Proterozoic metamorphic rocks as Nipton Hills [54], and hillslopes of upper elevations are mantled with similar colluvial deposits and associated soils as those at Nipton Hills (JRM, pers. obs.). Hillslopes above 2000 m asl in the McCullough Range contain pinyon and/or juniper on both south and north aspects (Figure 12A,B). Tree densities at these upper elevations are denser on north aspects, but even at these elevations, the woodlands are open with tree canopies covering only half the ground surface on the north aspect and less on the south, with herbaceous vegetation between canopies dominated by the perennial grasses *Bouteloua eriopoda*, *B. gracilis*, and *H. jamesii* (Figure 12C).

At the Nipton Hills study site, OSL ages of sediments incorporated within Bk and Btk horizons of the south-aspect colluvial remnant (Figure 6) indicate that by the end of the Pleistocene, soils with thick, fine-grained B horizons had developed within the coarse colluvial deposits. Wherever these kinds of soils had developed, perennial grasses with diffuse, fibrous root systems would probably have provided substantial ground cover in areas between widely spaced tree canopies on both north and south aspects, similar to what presently occurs at higher elevations in the McCullough Range. *Bouteloua gracilis* was likely the dominant grass species on the north aspects at the Nipton Hills site during the late Pleistocene, and probably also occurred on the south-aspect slopes together with both *H. jamesii* and *B. eriopoda*. This is similar to the vegetation composition commonly present at elevations above 1650 m asl in the nearby McCullough Range (Figure 12C) and New York Mountains. Since the distribution of plant species generally shifted upward in elevation 600–1000 m in response to the Pleistocene–Holocene climate transition, the present-day restriction of the more arid-adapted *H. rigida* to elevations below 1600 m asl suggests that it was probably absent from Nipton Hills during the late Pleistocene, but colonized the area during the more arid Holocene.

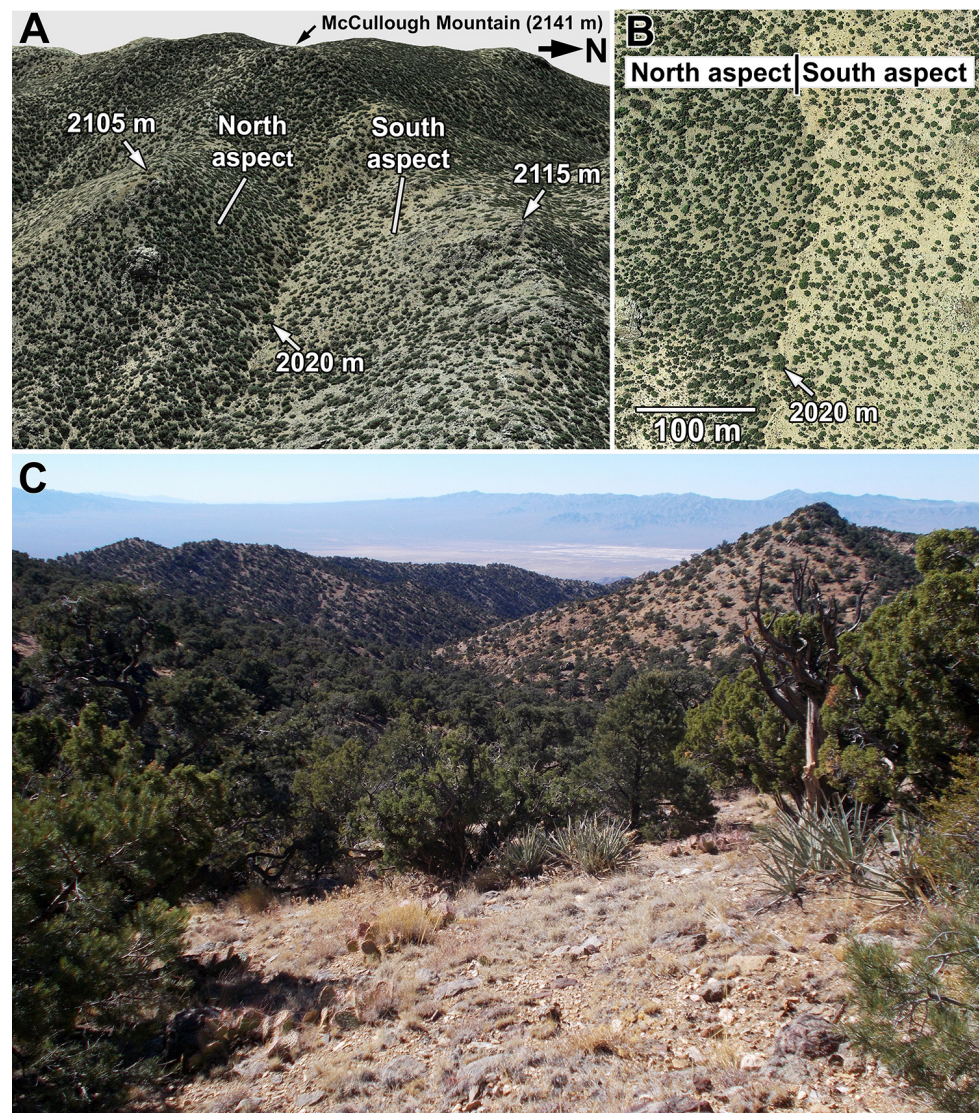


Figure 12. (A). Oblique aerial view (Google Earth Pro™) of the eastern slopes of the McCullough Range, 16 km N of the Nipton Hills study area showing pinyon-juniper woodlands on north and south aspect hillslopes. (B). Overhead, vertical aerial view of north versus south aspects on opposite sides of the channel shown in A. Neither aspect contains closed-canopy woodlands; tree canopies cover less than half the surface on the south aspect. (C). View toward the southwest from 2015 m asl in the McCullough Range showing perennial grasses (*Bouteloua gracilis*, *Hilaria jamesii*, and occasional *B. eriopoda*) occupying spaces between canopies of *Juniperus osteosperma* and *Pinus monophylla*. The sparsity of perennial grass cover in this view is due to an almost complete absence of warm-season precipitation during the summer of 2020; on the date of the photograph (30 October 2020) the grasses show no evidence of growth or flowering during that year. The sharp peak on the right, midground is 2002 m elev., and perennial grasses together with junipers similarly cover the hillslopes below that peak. Ivanpah Playa is visible on the floor of the basin in the background, approximately 20 km from the foreground location.

4.1.2. Initial Vegetation Transitions in the Early Holocene Driven by Climate Change

The palaeobotanical record clearly demonstrates the presence of pinyon-juniper or juniper woodlands during the late Pleistocene in all but the lowest elevations and most arid portions of what are now the Mojave and Sonoran Deserts [4]. The initial, direct response of vegetation to increasing aridity following the LPH was the retraction of those woodland elements to higher elevations. Using midden records compiled prior to 2005, [7] suggested a gradual, relatively linear, time-transgressive upward shift in elevation during the Holocene of the occurrence of junipers in the Mojave Desert between latitudes of 34° and 37° N. However, the poor constraint on the timing of vegetation change during the Holocene for elevations of 1100–1500 m asl (which includes the elevation range of the Nipton Hills site) due to the lack of midden records from 10 ka BP to 3 ka BP was also noted [7]. The inclusion of the additional midden records reported in [53] substantially increases the resolution of the timing of vegetation change over that elevation range and time interval (Figure 13). These additional records indicate that rather than a gradual upward retreat, junipers apparently disappeared over a wide range of elevations below 1500 m asl as early as 9 cal ka BP. We therefore conclude that at Nipton Hills, especially on the more xeric south-aspect hillslopes, junipers likely disappeared as early as 9–10 cal ka BP, well before the end of the early Holocene.

In the Nipton Hills, this vegetation change would have first occurred on the more xeric south aspect. Ultimately pinyon and juniper also disappeared from north-aspect hillslopes, since no woodrat midden records from this elevation in the Mojave Desert region indicate the presence of juniper (or pinyon) at this elevation past the time of the early Holocene (Figure 13). The direct effects of climatic aridification would probably have also affected the species composition, structure, and ground cover provided by perennial herbaceous vegetation, particularly the perennial grasses. However, despite the disappearance of juniper and pinyons by the end of the early Holocene, colluvial mantles and their associated soils apparently remained intact on both north and south-aspect hillslopes.

4.1.3. Subsequent Vegetation Transitions of the Middle-to Late Holocene

The record of alluvial deposition indicates that most soil erosion from south-aspect hillslopes apparently occurred around the end of the middle Holocene, several thousand years after pinyon and juniper trees disappeared. As long as thick, fine-grained soil horizons were present on both north and south-aspect hillslopes, those soils would have continued to support vegetation dominated by perennial grasses during the Holocene, as they do to the present day (Table 1 and Figure 10). Increased aridity during the middle Holocene in this part of the Mojave Desert [55], as well as throughout the entire Great Basin region [56], probably shifted species compositions of perennial grasses on south aspects to the more arid-adapted *Hilaria rigida*, from the likely dominance during the late Pleistocene and early Holocene of *H. jamesii* and *B. eriopoda*. A shift in dominance to *H. rigida*, with its lesser capacity to provide effective ground cover, would have decreased the connectivity of vegetation cover, thereby promoting increased runoff and erosion (Figure 10).

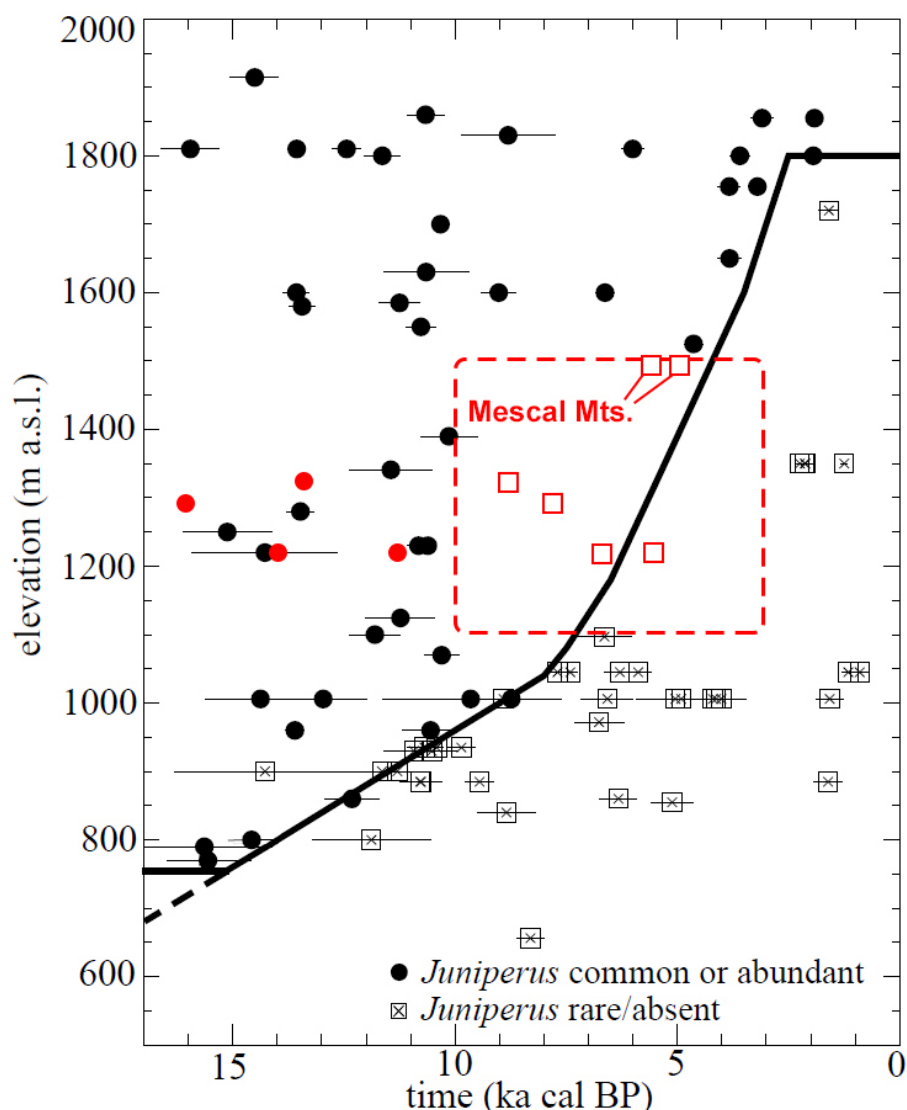


Figure 13. Relationship between elevation and the occurrence of junipers in fossil woodrat middens, modified from Figure 3 in [7] with additional information added in red. The solid black line is a boundary proposed in [7] that represents a gradual, time-transgressive upward shift in the distribution of *Juniperus* after the LP-H transition. The square outlined with a dashed red line indicates the elevation range (1100–1500 m) and time (10–3 ka) where the lack of midden records was noted, hence poor constraint on the timing of disappearance of juniper. Red symbols are records from [53] not included in [7]. Small open red squares within the large dashed red square represent middens lacking juniper; solid red circles are middens containing juniper. The two Mescal Mts. middens from [53] were from an elevation of 1490 m, 34 km west of Nipton Hills.

The second major phase of vegetation change during the Holocene apparently occurred once soils were eroded from south aspect hillslopes, leaving a substrate incapable of accommodating the diffuse, fibrous root systems of perennial grasses. Eroded portions of hillslopes were subsequently occupied by more xerophytic desert scrub vegetation—a sparse cover of desert shrubs and shallow-rooted succulents. The limited areas covered by perennial grasses that persist to this day on south-aspect hillslopes occur exclusively on the soils of small colluvial remnants of what originally was a more widespread mantle of thicker colluvium and associated soils. In contrast, on north-aspect hillslopes, the considerably denser perennial grass cover has largely prevented this kind of erosion throughout the Holocene. The vegetation transition on the more xeric south aspects from perennial grasses occupying deep soils in colluvium to sparse desert scrub after erosion of those soils may

have been most rapid towards the end of the mid Holocene and shortly thereafter. There was probably a lag of at least several thousand years between the first set of climate change-driven vegetation transitions during the early Holocene starting with the loss of pinyon and junipers, to those driven by soil erosion from south-aspect hillslopes around the time of the mid-late Holocene transition.

4.2. Climate, Vegetation Change, and Drivers of Fluvial System Behavior

The results of our investigations in the Nipton Hills bear directly on continuing debate regarding the degree to which vegetation governs the responses of fluvial systems in arid and semi-arid systems [7,57–59]. Ref. [58] proposed that greater effective moisture during the late Pleistocene supported vegetation that was sufficiently dense to favor increased weathering, formation of soils, and accumulation of colluvium on hillslopes. Increased aridity associated with the Pleistocene–Holocene transition reduced the magnitude of weathering, soil thickness, and vegetation density, which triggered erosion. The resulting sediment pulse overwhelmed fluvial systems, leading to fan deposition. As soils on hillslopes were progressively lost to erosion, exposing bedrock, sediment yields eventually diminished and runoff increased, switching fluvial system behavior from a phase of alluvial fan deposition to channel incision.

The universal applicability of the above model is debated. Refs. [40,58] argued for a reduced relevance of vegetation change as a major factor triggering hillslope sediment production and alluvial aggradation, and proposed a stronger role of marked changes in precipitation regimes [60]. However, the nearly complete stripping of soils from the sparsely vegetated south-aspect hillslopes, but lack of comparable erosion on more densely vegetated, north-aspect hillslopes at Nipton Hills, demonstrates the strong role played by vegetation in modulating erosion, sediment supply, and fluvial system responses.

Vegetation change following the LPH involving the loss of pinyon and juniper as indicated by records from ancient woodrat middens has been implicitly regarded as the kind of change associated with increased erosion and sediment production [7,58]. However, in the Nipton Hills, the retention of colluvial mantles and soils on the mesic north-aspect hillslopes throughout the Holocene demonstrates that the disappearance of pinyon and juniper by themselves was not the principal driver of erosion. Instead, the persistence of a relatively dense cover of perennial herbaceous vegetation, particularly perennial C₄ grasses, long after the disappearance of trees, apparently played a much larger role in governing surface hydrological responses and sediment yield.

4.3. Landscape Responses along Gradients of Precipitation Amount and Seasonality

Monsoonal precipitation declines markedly in the Mojave Desert to the west of the Nipton Hills, and C₄ perennial grasses correspondingly decline as significant components of the vegetation [61]. For example, the western distributional limit of *Bouteloua eriopoda* is 40 km west of Nipton Hills [24]. Even within areas receiving substantial summer precipitation in the eastern Mojave Desert and further eastward into the Sonoran Desert region of southern Arizona, total annual precipitation declines with elevation. The consequence of this overall decline is also a reduced representation of perennial C₄ grasses and a corresponding transition to shrub-dominated desert scrub vegetation in response to increasing aridity. In semi-arid environments of the American Southwest, perennial C₄ grasses are intimately associated with soils that support their diffuse, fibrous root systems [24,45]. In those soil environments, the ground cover typically provided by perennial C₄ grasses is far more effective at impeding overland flow and erosion than is the patchy cover provided by woody shrubs [62–64]. Consequently, significant differences in landscape behavior within the region would be expected to occur along gradients of climate and characteristic vegetation (east to west with declining monsoonal inputs; high to low elevations with diminishing total precipitation).

Studies of alluvial fan deposits and fluvial system behavior in the Mojave Desert region have largely been conducted further to the west or lower in elevation in landscapes

lacking the substantial perennial grass component present at Nipton Hills. This may be a significant contributor to differences reported in late Quaternary landscape behavior, particularly the absence at the Nipton Hills of a prominent record of sediment production and alluvial fan deposition around the time of the LPH. That absence contrasts with studies of the piedmont of the Soda Mountains [65] and the piedmont of the western side of the Providence Mountains [40], located 90 km W and 70 km SW, respectively, of the Nipton Hills. In those areas, fan deposits dated to the time of the LPH are substantial and voluminous, consisting of debris flows and alluvial sediments that form prominent geomorphic surfaces into which younger Holocene deposits are inset. The enigmatic absence of a prominent LPH deposit in the sedimentary record of Nipton Hills is most plausibly explained by the capacity of considerably denser, perennial grass-dominated vegetation on both north- and south-aspect hillslopes to inhibit soil erosion at that time. In contrast, the piedmont of the Soda Mountains is at a considerably lower, more arid elevation (300–400 m asl), and hillslopes there are unlikely to have been occupied by relatively dense cover of perennial grasses during the late Pleistocene. Comparison of the late Quaternary records of the Nipton Hills site to those on the west side of the Providence Mountains is complicated because of large areas of sparsely vegetated hillslopes at the latter below 1100 m asl, combined with the considerably larger areas of steeper and much higher elevation (and correspondingly larger drainage basins generating greater runoff) than in the Nipton Hills.

Our work in Nipton Hills, as well as investigations in other arid regions of the world (e.g., [59]) indicate that the responses of landscapes to the LPH have been more complex and varied in space and time than that proposed in [57]. Nevertheless, that model has and continues to provide a valuable framework and point of departure for further investigations of landscape responses to past climate change as well as to various anthropogenic changes experienced now and in the future.

4.4. Predominant Climate Drivers of Landscape Change

Although increasing aridity after the LPH initiated major vegetation changes, other climatic perturbations were likely required to initiate the magnitude of hillslope erosion, sediment transport and deposition responsible for episodes of alluvial fan aggradation. Compiled records of age-constrained, late Quaternary alluvial-fan deposits in the Mojave Desert indicate two predominant periods of alluvial aggradation—one bracketing the LPH from 14–9 ka BP, and another from 6–3 ka BP [66]. Although the Nipton Hills study area apparently lacks a record of a major alluvial deposition during the earlier period, the age of the mid-late Holocene terrace is synchronous with the more recent one. This synchronous timing strongly points to a common climate signal in the form of region-wide occurrence of storms of with intensity and duration capable of generating the runoff and sediment pulses required for alluvial transport and fan deposition.

Increased frequency and intensity of monsoonal storms have been proposed as the principal driver of these depositional episodes [57,66]. However, other climate phenomena more capable of delivering the heavy and sustained precipitation over geographically widespread areas may have been involved, for example the incursion of eastern Pacific tropical cyclonic storms into the region associated with El Niño conditions. Multiple proxy climate records (marine sediment cores and Andean lake sediment cores) indicate enhanced El Niño precipitation regimes that coincide with the periods of increased alluvial fan deposition in the Mojave Desert [60,67,68]. There is also evidence that the El Niño warm phase of the ENSO cycle discharges heat into the eastern North Pacific basin months after its typical wintertime peak, intensifying eastern north Pacific tropical cyclones as a result [69]. Historical precipitation records from the southwestern USA show that El Niño conditions resulted in normal to above-normal warm-season precipitation, a significant portion of it from dissipating tropical cyclones [70]. In pinyon-juniper vegetation at a site in northeastern Arizona, a historically recent episode of extreme hillslope erosion in a pinyon-juniper woodland in the early 1900s was linked to three region-wide episodes of substantial

rainfall in October, 1907 that were interpreted as incursions of Pacific tropical cyclones [71]. We agree with [60] that increases in tropical Pacific cyclonic storm activity likely contributed significantly to the regionally synchronous, late Quaternary fluvial behavior in the Mojave Desert region. However, the contrasting behaviors of north- and south-aspect hillslopes at Nipton Hills nevertheless demonstrate substantial variation in responses to climate signals, as a function of vegetation cover.

4.5. Effects of Future Climate Change

For the semi-arid setting of Nipton Hills, the ecological transition from open woodlands containing pinyon pine and juniper in the late Pleistocene to sparse Mojave desert scrub cannot be understood simply as a function of direct responses of plants and vegetation to climate. Major climate change at the LPH, as well as smaller changes during the Holocene generated a complex cascade of responses involving both biotic and physical components of the environment. The overall contrast in the present-day vegetation of north and south-aspect hillslopes (e.g., Figures 1 and 2) is only partly explained as a function of strong topoclimatic contrasts driven by differences in insolation and evapotranspiration. The present-day existence of two very different kinds of vegetation on the xeric south aspects—one dominated by perennial grasses, the other by sparse Mojave desert scrub—underscores how contrasting soil characteristics modulate a common climate signal by creating different soil hydrologic conditions capable of supporting different kinds of plants [45]. The spatial distribution of those soil conditions has not been static since the LPH, but has changed as erosion has radically altered the spatial and temporal distribution of plant available moisture over the landscape.

The prominent terrace composed of mid-late Holocene alluvium derived principally from materials eroded from south-aspect hillslopes suggests that a critical threshold of vegetation cover required to inhibit erosion on those hillslopes was crossed. When such occurs, strong, self-reinforcing feedback between responses of biotic and physical components of the landscape frequently leads to irreversible changes in arid and semi-arid environments on a time scale relevant to use of landscapes by people [57,62]. Responses of drylands to environmental perturbations (both climate change and land-use practices) frequently occur in a series of nonlinear thresholds that once passed, lead to irrecoverable ecosystem change: (1) a phase of vegetation decline, (2) a resulting soil disruption phase, which leads to further vegetation changes, and in the most extreme cases, (3) a systemic breakdown of ecosystem function [72]. The environmental transitions that occurred during the Holocene on south-aspect hillslopes at Nipton Hills represent those first two stages.

Detailed knowledge of environmental responses to climate change during the late Quaternary can help increase the understanding of possible future scenarios and trajectories of ecological and landscape changes. For example, the type and amount of vegetation cover currently present on north-aspect hillslopes at the Nipton Hills has apparently been sufficient to protect and maintain much of the soil mantle upon which that vegetation depends. The diminished vegetation cover on similar soils of the south-aspect hillslopes (Figure 10) could not perform the same function. Consequently, the threshold separating the two very different responses of south and north-aspect hillslopes lies between those two amounts of vegetation cover. Any future change, either driven by climate or land use, that diminishes the cover on north-aspect hillslopes would move those environments closer to an apparent threshold where irreversible soil losses and associated vegetation changes could be initiated. By extension, at higher elevations of other nearby locales, south-aspect hillslopes presently maintain sufficient density and cover of perennial grass-dominated vegetation to hold underlying soils in place. Increasing temperatures and reduced plant-available moisture could likewise move those hillslopes beyond a threshold where undesirable alterations of the soil environment and vegetation could occur.

5. Conclusions

Predicting the ecological consequences of future climate change in arid and semi-arid regions requires identification and understanding of thresholds that separate starkly different domains of hydrologic behavior and vegetation responses. Computational tools like climate envelope modeling cannot in themselves predict the cascade of interactions and changes in the biotic and physical environment that ultimately will likely determine the timing and spatial extent of many vegetation changes in the future, particularly in the world's dryland environments. Such approaches use knowledge of current distributions of species with respect to climate variables to predict future geographic distributions of species and vegetation in changed climate regimes. Although some approaches in species distribution modeling include information on soil conditions, they are unable to predict the kinds of landscape responses and changes in the soil environment that may occur simultaneously and consequently affect distributions of species and vegetation. In arid and semi-arid regions, some of the largest ecological consequences of future climate change may not be due to the direct effects of climate per se on organisms, but rather the way relatively minor biotic changes driven initially by climate can set even greater landscape-changing processes and even more extreme biotic change in motion.

Author Contributions: Conceptualization, J.R.M., L.D.M. and L.P.P.; Methodology, J.R.M., L.D.M., L.P.P. and T.M.R.; Field investigations and sample collection, J.R.M., L.D.M. and L.P.P.; OSL dating, T.M.R.; writing—original draft preparation, J.R.M.; writing—review and editing, L.D.M., L.P.P. and T.M.R.; funding acquisition, J.R.M., L.D.M. and L.P.P. All authors have read and agreed to the published version of the manuscript.

Funding: Funding was provided by the Desert Botanical Garden, the University of New Mexico, Whitman College, and the Geological Society of America Gladys Cole Memorial Research Award to LPP.

Data Availability Statement: Data pertaining to soil profile descriptions and OSL dating results are found in [22] (supporting materials). Data pertaining to vegetation data are reported directly in this paper.

Acknowledgments: In 2004, Tony L. Burgess accompanied J.R.M. on an initial examination of the site and collection of preliminary information on vegetation and soils, which eventually led to this investigation. Many people assisted during the research conducted from 2014 to 2020. Lucas Majure accompanied J.R.M. on long-distance reconnaissance on foot of the entire Nipton Hills area, ranging from the southern to the northern drainage basins. Veronica Nixon provided high-resolution, color print images of infrared imagery used for vegetation mapping. Several Whitman College students assisted with various aspects of fieldwork including Saisha Brody, Sarah Dunn, Addison Richter, Tara Stahlecker, and Christopher Suhr. Tara Stahlecker and M. Nelson assisted with OSL analyses.

Conflicts of Interest: The authors declare no conflict of interest.

References

1. Wells, P.V.; Jorgensen, C.D. Pleistocene wood rat middens and climatic change in Mohave Desert: A record of juniper woodlands. *Science* **1964**, *143*, 1171–1173. [[CrossRef](#)] [[PubMed](#)]
2. Wells, P.V.; Berger, R. Late Pleistocene history of coniferous woodland in the Mojave Desert. *Science* **1967**, *155*, 1640–1647. [[CrossRef](#)] [[PubMed](#)]
3. King, T.J., Jr. Late Pleistocene—Early Holocene history of coniferous woodlands in the Lucerne Valley region, Mohave desert, California. *Gr. Basin Nat.* **1976**, *36*, 227–238.
4. Betancourt, J.L.; Van Devender, T.R.; Martin, P.S. (Eds.) *Packrat Middens: The Last 40,000 Years of Biotic Change*; University of Arizona Press: Tucson, AZ, USA, 1990.
5. Spaulding, W.G. Vegetational and climatic development of the Mojave Desert: The last glacial maximum to the present. In *Packrat Middens: The Last 40,000 Years of Biotic Change*; Betancourt, J.L., Van Devender, T.R., Martin, P.S., Eds.; University of Arizona Press: Tucson, AZ, USA, 1990; pp. 166–199.
6. Harvey, A.M.; Wigand, P.E.; Wells, S.G. Response of alluvial fan systems to the late Pleistocene to Holocene climatic transition: Contrasts between the margins of pluvial Lakes Lahontan and Mojave, Nevada and California, USA. *Catena* **1999**, *36*, 255–281. [[CrossRef](#)]

7. Pelletier, J.D. The linkages among hillslope-vegetation changes, elevation, and the timing of late-Quaternary fluvial-system aggradation in the Mojave Desert revisited. *Earth Surf. Dyn.* **2014**, *2*, 455–468. [[CrossRef](#)]
8. Davis, M.B.; Woods, K.D.; Webb, S.L.; Futyma, R.P. Dispersal versus climate: Expansion of *Fagus* and *Tsuga* into the Upper Great Lakes region. *Vegetatio* **1986**, *67*, 93–103. [[CrossRef](#)]
9. McAuliffe, J.R.; Van Devender, T.R. A 22,000-year record of vegetation change in the north-central Sonoran Desert. *Palaeogeog. Palaeoclim. Palaeoecol.* **1998**, *141*, 253–275. [[CrossRef](#)]
10. Cole, K. Past rates of change, species richness, and a model of vegetational inertia in the Grand Canyon, Arizona. *Amer. Nat.* **1985**, *125*, 289–303. [[CrossRef](#)]
11. Cole, K.L. In defense of inertia. *Amer. Nat.* **1986**, *127*, 727–728. [[CrossRef](#)]
12. McFadden, L.D.; Wells, S.G.; Jercinovich, M.J. Influences of eolian and pedogenic processes on the origin and evolution of desert pavements. *Geology* **1987**, *15*, 504–508. [[CrossRef](#)]
13. Adelsberger, K.A.; Smith, J.R. Desert pavement development and landscape stability on the Eastern Libyan Plateau, Egypt. *Geomorphology* **2009**, *107*, 178–194. [[CrossRef](#)]
14. McDonald, E.V.; Pierson, F.B.; Flerchinger, G.N.; McFadden, L.D. Application of a soil-water balance model to evaluate the influence of Holocene climate change on calcic soils, Mojave Desert, California, USA. *Geoderma* **1996**, *74*, 167–192. [[CrossRef](#)]
15. Meadows, D.G.; Young, M.H.; McDonald, E.V. Influence of relative surface age on hydraulic properties and infiltration on soils associated with desert pavements. *Catena* **2008**, *72*, 169–178. [[CrossRef](#)]
16. McAuliffe, J.R.; McDonald, E.V. Holocene environmental change and vegetation contraction in the Sonoran Desert. *Quat. Res.* **2006**, *65*, 204–215. [[CrossRef](#)]
17. McAuliffe, J.R. Soil horizon development and the tempo and modes of vegetation change during the Holocene in a Sonoran Desert basin, USA. *Holocene* **2019**, *29*, 1263–1272. [[CrossRef](#)]
18. McAuliffe, J.R. The Sonoran Desert: Landscape complexity and ecological diversity. In *Ecology of Sonoran Desert Plants and Plant Communities*; Robichaux, R., Ed.; University of Arizona Press: Tucson, AZ, USA, 1999; pp. 87–104.
19. McAuliffe, J.R. Desert soils. In *A Natural History of the Sonoran Desert*, 2nd ed.; Dimmitt, M.A., Comas, P.W., Brewer, L.M., Eds.; Arizona-Sonora Desert Museum Press & Univ. of California Press: Berkeley, CA, USA, 2015; pp. 85–100.
20. McAuliffe, J.R.; Sundt, P.C.; Valiente-Banuet, A.; Casas, A.; Viveros, J.L. Pre-Columbian soil erosion, persistent ecological changes, and collapse of a subsistence agricultural economy in the semi-arid Tehuacán Valley, Mexico’s “Cradle of Maize”. *J. Arid Environ.* **2001**, *47*, 47–75. [[CrossRef](#)]
21. McAuliffe, J.R.; McFadden, L.D.; Roberts, L.M.; Wawrzyniec, T.F.; Scuderi, L.A.; Meyer, G.A.; King, M.P. Non-equilibrium hillslope dynamics and irreversible landscape changes at a shifting pinyon-juniper woodland. *Glob. Planet. Chang.* **2014**, *122*, 1–13. [[CrossRef](#)]
22. Persico, L.; McFadden, L.; McAuliffe, J.; Rittenour, T.; Stahlecker, T.; Dunn, S.; Brody, W. Late Quaternary geochronologic record of soil formation and erosion: Effects of climate change on Mojave Desert hillslopes. *Geology* **2021**, *50*, 54–59. [[CrossRef](#)]
23. Miller, D.M. *Surficial geologic map of the Ivanpah 30' × 60' Quadrangle, San Bernardino County, California, and Clark County, Nevada: U.S. Geological Survey Scientific Investigations Map 3206, Scale 1:100,000*; U.S. Geological Survey: Menlo Park, CA, USA, 2012; 14p.
24. McAuliffe, J.R. Perennial Grass-Dominated Plant Communities of the Eastern Mojave Desert Region. *Desert Plants* **2016**, *32*, 1–90. Available online: <https://repository.arizona.edu/handle/10150/622004> (accessed on 1 January 2020).
25. Rowlands, P.; Johnson, H.; Ritter, E.; Endo, A. The Mojave desert. In *Reference Handbook on the Deserts of North America*; Bender, G.L., Ed.; Greenwood Press: Westport, London, UK, 1982; pp. 103–162.
26. Corbosiero, K.L.; Dickinson, M.J.; Bosart, L.F. The contribution of eastern North Pacific tropical cyclones to the rainfall climatology of the southwest United States. *Mon. Weather Rev.* **2009**, *137*, 2415–2435. [[CrossRef](#)]
27. Ritchie, E.A.; Wood, K.M.; Gutzler, D.S.; White, S.R. The influence of eastern Pacific tropical cyclone remnants on the southwestern United States. *Mon. Weather Rev.* **2011**, *139*, 192–210. [[CrossRef](#)]
28. Walker, M.; Head, M.J.; Lowe, J.; Berkelhammer, M.; Björck, S.; Cheng, H.; Cwynar, L.C.; Fisher, D.; Gkinis, V.; Long, A.; et al. Subdividing the Holocene Series/Epoch: Formalization of stages/ages and subseries/subepochs, and designation of GSSPs and auxiliary stratotypes. *J. Quat. Sci.* **2019**, *34*, 173–186. [[CrossRef](#)]
29. Gile, L.H.; Peterson, F.F.; Grossman, R.B. Morphological and genetic sequences of carbonate accumulation in desert soils. *Soil Sci.* **1966**, *101*, 347–360. [[CrossRef](#)]
30. Reheis, M.C.; Goodmacher, J.C.; Harden, J.W.; McFadden, L.D.; Rockwell, T.K.; Shroba, R.R.; Sowers, J.M.; Taylor, E.M. Quaternary soils and dust deposition in southern Nevada and California. *Geol. Soc. Amer. Bull.* **1995**, *107*, 1003–1022. [[CrossRef](#)]
31. Ugolini, F.C.; Hillier, S.; Certini, G.; Wilson, M.J. The contribution of aeolian material to an Aridisol from southern Jordan as revealed by mineralogical analysis. *J. Arid Environ.* **2008**, *72*, 1431–1447. [[CrossRef](#)]
32. Hirmas, D.R.; Graham, R.C.; Kendrick, K.J. Pedogenesis and soil-geomorphic relationships in an arid mountain range, Mojave Desert, California. *Soil Sci. Soc. Amer. J.* **2011**, *75*, 192–206. [[CrossRef](#)]
33. Hirmas, D.R.; Graham, R.C.; Kendrick, K.J. Soil-geomorphic significance of lands surface characteristics in an arid mountain range, Mojave Desert, USA. *Catena* **2011**, *87*, 408–420. [[CrossRef](#)]
34. Persico, L.P.; McFadden, L.D.; Frechette, J.D.; Meyer, G.A. Rock type and dust influx control accretionary soil development on hillslopes in the Sandia Mountains, New Mexico, USA. *Quat. Res.* **2011**, *76*, 411–416. [[CrossRef](#)]

35. Goossens, D. Field experiments of aeolian dust accumulation on rock fragment substrata. *Sedimentology* **1995**, *42*, 391–402. [[CrossRef](#)]
36. Blank, R.R.; Young, J.A.; Lugaski, T. Pedogenesis on talus slopes, the Buckskin range, Nevada, USA. *Geoderma* **1996**, *71*, 121–142. [[CrossRef](#)]
37. Chadwick, O.A.; Davis, J.O. Soil-forming intervals caused by eolian sediment pulses in the Lahontan basin, northwestern Nevada. *Geology* **1990**, *18*, 243–246. [[CrossRef](#)]
38. Reheis, M.C.; Kihl, R. Dust deposition in southern Nevada and California, 1984–1989: Relations to climate, source area, and source lithology. *J. Geophys. Res. Atmos.* **1995**, *100*, 8893–8918. [[CrossRef](#)]
39. Sweeney, M.R.; McDonald, E.V.; Etyemezian, V. Quantifying dust emissions from desert landforms, eastern Mojave Desert, USA. *Geomorphology* **2011**, *135*, 21–34. [[CrossRef](#)]
40. McDonald, E.V.; McFadden, L.D.; Wells, S.G.; Enzel, Y.; Lancaster, N. Regional response of alluvial fans to the Pleistocene–Holocene climatic transition, Mojave Desert, California. In *Paleoenvironments and Paleohydrology of the Mojave and Southern Great Basin Deserts*; Enzel, Y., Wells, S.G., Lancaster, N., Eds.; Geological Society of America: Boulder, CO, USA, 2003; Volume 368, pp. 189–205.
41. Yan, Y.; Xu, X.; Xin, X.; Yang, G.; Wang, X.; Yan, R.; Chen, B. Effect of vegetation coverage on aeolian dust accumulation in a semiarid steppe of northern China. *Catena* **2011**, *87*, 351–356. [[CrossRef](#)]
42. Vasek, F.C. Creosote bush: Long-lived clones in the Mojave Desert. *Am. J. Bot.* **1980**, *67*, 246–255. [[CrossRef](#)]
43. McAuliffe, J.R.; Hamerlynck, E.P.; Eppes, M.C. Landscape dynamics fostering the development and persistence of long-lived creosotebush (*Larrea tridentata*) clones in the Mojave Desert. *J. Arid Environ.* **2007**, *69*, 96–126. [[CrossRef](#)]
44. Helms, J.G.; McGill, S.F.; Rockwell, T.K. Calibrated, late Quaternary age indices using clast rubification and soil development on alluvial surfaces in Pilot Knob Valley, Mojave Desert, southeastern California. *Quat. Res.* **2003**, *60*, 377–393. [[CrossRef](#)]
45. McAuliffe, J.R. The interface between precipitation and vegetation: The importance of soils in arid and semiarid environments. In *Changing Precipitation Regimes and Terrestrial Ecosystems: A North American Perspective*; Weltzin, J., McPherson, G.R., Eds.; University of Arizona Press: Tucson, AZ, USA, 2003; pp. 9–27.
46. Sternberg, P.D.; Anderson, M.A.; Graham, R.C.; Beyers, J.L.; Tice, K.R. Root distribution and seasonal water status in weathered granitic bedrock under chaparral. *Geoderma* **1996**, *72*, 89–98. [[CrossRef](#)]
47. Noy-Meir, I. Desert ecosystems: Environment and producers. *Annu. Rev. Ecol. Syst.* **1973**, *4*, 25–51. [[CrossRef](#)]
48. Witty, J.H.; Graham, R.C.; Hubbert, K.R.; Doolittle, J.A.; Wald, J.A. Contributions of water supply from the weathered bedrock zone to forest soil quality. *Geoderma* **2003**, *114*, 389–400. [[CrossRef](#)]
49. McCormick, E.L.; Dralle, D.N.; Hahm, W.J.; Tune, A.K.; Schmidt, L.M.; Chadwick, K.D.; Rempe, D.M. Widespread Woody Plant Use of Water Stored in Bedrock. *Nature* **2021**, *597*, 225–229. Available online: <https://www.fs.fed.us/psw/publications/dralle/psw2021dralle005mccormick.pdf> (accessed on 1 January 2020). [[CrossRef](#)] [[PubMed](#)]
50. Sala, O.E.; Lauenroth, W.K.; Golluscio, R.A. Plant functional types in temperate semi-arid areas. In *Plant Functional Types*; Smith, T.M., Shugart, H.H., Woodward, F.I., Eds.; Cambridge University Press: Cambridge, UK, 1997; pp. 217–233.
51. Schenk, H.J.; Jackson, R.B. Rooting depths, lateral root spreads and below-ground/above-ground allometries of plants in water-limited ecosystems. *J. Ecol.* **2002**, *90*, 480–494. [[CrossRef](#)]
52. Holmgren, C.A.; Betancourt, J.L.; Rylander, K.A. A long-term vegetation history of the Mojave–Colorado desert ecotone at Joshua Tree National Park. *J. Quat. Sci.* **2010**, *25*, 222–236. [[CrossRef](#)]
53. Koehler, P.A.; Anderson, R.S.; Spaulding, W.G. Development of vegetation in the central Mojave Desert of California during the late Quaternary. *Palaeogeogr. Palaeoclim. Palaeoecol.* **2005**, *215*, 297–311. [[CrossRef](#)]
54. Longwell, C.R.; Pampeyan, E.H.; Bowyer, B.; Roberts, R.J. *Geology and Mineral Deposits of Clark County, Nevada*; Nevada Bureau of Mines and Geology Bulletin 62; Mackay School of Mines, University of Nevada-Reno: Reno, NV, USA, 1965.
55. Spaulding, W.G. A middle Holocene vegetation record from the Mojave Desert of North America and its paleoclimatic significance. *Quat. Res.* **1991**, *35*, 427–437. [[CrossRef](#)]
56. Steponaitis, E.; Andrews, A.; McGee, D.; Quade, J.; Hsieh, Y.T.; Broecker, W.S.; Shuman, B.N.; Burns, S.J.; Cheng, H. Mid-Holocene drying of the US Great Basin recorded in Nevada speleothems. *Quat. Sci. Rev.* **2015**, *127*, 174–185. [[CrossRef](#)]
57. Bull, W.B. *Geomorphic Responses to Climate Change*; Oxford University Press: Oxford, UK, 1991.
58. Antinao, J.L.; McDonald, E. A reduced relevance of vegetation change for alluvial aggradation in arid zones. *Geology* **2013**, *41*, 11–14. [[CrossRef](#)]
59. Enzel, Y.; Amit, R.; Grodek, T.; Ayalon, A.; Lekach, J.; Porat, N.; Bierman, P.; Blum, J.D.; Erel, Y. Late Quaternary weathering, erosion, and deposition in Nahal Yael, Israel: An “impact of climatic change on an arid watershed”? *Geol. Soc. Amer. Bull.* **2012**, *124*, 705–722. [[CrossRef](#)]
60. Antinao, J.L.; McDonald, E. An enhanced role for the Tropical Pacific on the humid Pleistocene–Holocene transition in southwestern North America. *Quat. Sci. Rev.* **2013**, *78*, 319–341. [[CrossRef](#)]
61. Johnson, H.B. Vegetation and plant communities of southern California deserts—A functional view. In *Plant Communities of Southern California*; Latting, J., Ed.; Special Publication No. 2; California Native Plant Society: Sacramento, CA, USA, 1976; pp. 125–164.
62. Schlesinger, W.H.; Reynolds, J.F.; Cunningham, G.L.; Huenneke, L.F.; Jarrell, W.M.; Virginia, R.M.; Whitford, W.G. Biological feedbacks in global desertification. *Science* **1990**, *247*, 1043–1048. [[CrossRef](#)]

63. Abrahams, A.D.; Parsons, A.J.; Wainwright, J. Effects of vegetation change on interrill runoff and erosion, Walnut Gulch, southern Arizona. *Geomorphology* **1995**, *13*, 37–48. [[CrossRef](#)]
64. Gutiérrez-Jurado, H.A.; Vivoni, E.R.; Cikowski, C.; Harrison, J.B.; Bras, R.L.; Istanbuloglu, E. On the observed ecohydrological dynamics of a semiarid basin with aspect delimited ecosystems. *Water Resour. Res.* **2013**, *49*, 8263–8284. [[CrossRef](#)]
65. Wells, S.G.; McFadden, L.D.; Dohrenwend, J.C. Influence of late Quaternary climatic changes on geomorphic and pedogenic processes on a desert piedmont, eastern Mojave Desert, California. *Quat. Res.* **1987**, *27*, 130–146. [[CrossRef](#)]
66. Miller, D.M.; Schmidt, K.M.; Mahan, S.A.; McGeehin, J.P.; Owen, L.A.; Barron, J.A.; Lehmkuhl, F.; Löhner, R. Holocene landscape response to seasonality of storms in the Mojave Desert. *Quat. Internat.* **2010**, *215*, 45–61. [[CrossRef](#)]
67. Rein, B.; Lückge, A.; Reinhardt, L.; Sirocko, F.; Wolf, A.; Dullo, W.C. El Niño variability off Peru during the last 20,000 years. *Paleoceanography* **2005**, *20*, PA4003. Available online: <https://agupubs.onlinelibrary.wiley.com/doi/pdf/10.1029/2004PA001099> (accessed on 1 January 2022). [[CrossRef](#)]
68. Moy, C.M.; Seltzer, G.O.; Rodbell, D.T.; Anderson, D.M. Variability of El Niño/Southern Oscillation activity at millennial timescales during the Holocene epoch. *Nature* **2002**, *420*, 162–165. [[CrossRef](#)]
69. Jin, F.F.; Boucharel, J.; Lin, I.I. Eastern Pacific tropical cyclones intensified by El Niño delivery of subsurface ocean heat. *Nature* **2014**, *516*, 82–85. [[CrossRef](#)] [[PubMed](#)]
70. Hereford, R.; Webb, R.H. Historic variation of warm-season rainfall, southern Colorado Plateau, southwestern USA. *Clim. Chang.* **1992**, *22*, 239–256. [[CrossRef](#)]
71. McAuliffe, J.R.; Scuderi, L.A.; McFadden, L.D. Tree-ring record of hillslope soil erosion and valley floor dynamics: Landscape responses to climate variation during the last 400 years in the Colorado Plateau, northeastern Arizona. *Glob. Planet. Chang.* **2006**, *50*, 184–201. [[CrossRef](#)]
72. Berdugo, M.; Delgado-Baquerizo, M.; Soliveres, S.; Hernández-Clemente, R.; Zhao, Y.; Gaitán, J.J.; Gross, N.; Saiz, H.; Maire, V.; Lehman, A.; et al. Global ecosystem thresholds driven by aridity. *Science* **2020**, *367*, 787–790. [[CrossRef](#)] [[PubMed](#)]